Physics – Uspekhi **52** (1) 55 – 77 (2009)

INSTRUMENTS AND METHODS OF INVESTIGATION PACS numbers: 42.65.Ky, 42.79.Nv, **52.38. – r**

Generation of high-order harmonics of high-power lasers in plasmas produced under irradiation of solid target surfaces by a prepulse

R A Ganeev

DOI: 10.3367/UFNe.0179.200901c.0065

Contents

Abstract. Research on high-order harmonic generation in laser-produced plasmas is reviewed. We analyze the conditions for the generation of harmonics (up to the 101st order, $\lambda = 7.9$ nm) in the propagation of laser radiation through a weakly ionized plasma prepared by irradiating the surfaces of different targets with a laser prepulse. We discuss the findings of investigations into the resonance intensity enhancement of individual harmonics in a number of plasma formations, which have demonstrated a substantial increase in the conversion efficiency in the plateau region of the harmonic-order distribution (in particular, of the 13th harmonic in indium plasmas with the efficiency 10^{-4}). We review the results of investigations of harmonic generation in nanoparticle-containing plasmas. Different techniques for increasing the intensity and order of the generated harmonics are discussed.

1. Introduction

High-order harmonic generation (HHG) may presently be considered the simplest and most efficient technique of obtaining coherent short-wavelength radiation in a broad spectral range [1 – 9]. Alternative means in this area are the use of X-ray lasers [10, 11] and free-electron lasers [12]. However, unlike sources involving harmonic generation, X-ray lasers have been unable to generate radiation in a broad range of the extreme ultraviolet (XUV) spectral domain. Other disadvantages of X-ray lasers are their poor spatial coherence and radiation divergence. As regards free-electron lasers that generate radiation in the XUV spectral range, there are only a few reports about the operation of these devices, which are limited in number. Furthermore, the application of these lasers is largely limited by their high cost.

HHG research is actively being pursued due to the availability of new high-power compact laser systems offering high output parameters (high energy and intensity of pulses and a high pulse repetition rate). Two mechanisms are used for HHG: harmonic generation in gases [1, 3 – 7] and from surfaces [2, 8, 9]. The considerable progress achieved in this area has enabled extending the range of generated coherent radiation to the spectral region where the radiation can pass through water-bearing components (the so-called water window, 2.3 – 4.6 nm [6, 7]). This circumstance is attractive from the standpoint of the practical use of coherent short-wavelength radiation in studies of biological objects. However, the data on the generation of such radiation obtained to date with the use of the above techniques have exhibited a low efficiency of conversion to the XUV range (10^{-5} and below), which considerably limits their practical use. This is supposedly the reason why in the last few years, the emphasis has been placed on the optimization of another effect discovered in these investigations, the generation of attosecond pulses (see review [13]).

R A Ganeev Akadempribor Research and Production Association, Academy of Sciences of Uzbekistan, Tashkent, Uzbekistan, ul. F Khodzhaeva 28, Akademgorodok, 100125 Tashkent, Uzbekistan
Tel. (998) 71 262 13 45
E-mail: rashid_ganeev@mail.ru

Received 24 April 2008, revised 15 August 2008
Uspekhi Fizicheskikh Nauk **179** (1) 65 – 90 (2009)
DOI: 10.3367/UFNr.0179.200901c.0065
Translated by E N Ragozin; edited by A M Semikhatov

The search for ways of increasing the HHG efficiency in the XUV spectral range has long been (and still is) among the most topical problems of nonlinear optics. However, in the majority of cases, the efficiency of conversion to high-order harmonics turns out to be insufficient for using them as real coherent short-wavelength radiation sources in biology, plasma diagnostics, medicine, microscopy, photolithography, etc. The feasibility of increasing the intensities of high-order harmonics generated in gas-jet sources by using atomic and ion resonances has been studied primarily by theoretical methods [14, 15]. The results of a number of calculations suggest that the intensity of a harmonic may be substantially increased when this harmonic is at resonance with transitions in the atomic and ion spectra of gases. This approach may be an alternative (or a complement) to the method of wave phase matching for harmonics and laser radiation used in Refs [6, 7].

The first experiments on HHG in the passage of laser radiation through a plasma produced at the surface of a solid target turned out to be much less successful. As noted in a recently published review on the bifurcational properties of harmonics in plasmas, "the effect of harmonic generation (in plasmas) calls for a more careful consideration and an in-depth basic research" [16]. Data obtained with the use of highly excited plasmas containing multiply charged ions revealed several limiting factors, which did not permit generating harmonics of a sufficiently high order [17 – 22]. Moreover, the harmonic intensity distribution did not correspond to the so-called three-stage HHG model [23], according to which a plateau-like high-order harmonic intensity distribution (i.e., of approximately equal intensity) should be observed. These investigations, which were carried out in the mid-1990s, stopped at the demonstration of relatively low-order harmonics (from the 11th through the 26th) (see Section 9, Fig. 20). These disadvantages, as well as the low conversion efficiency, led to the erosion of interest in this HHG technique, especially in comparison with the achievements involving gas-jet sources.

Nevertheless, there is reason to hope that harmonic intensities may be increased and shorter-wavelength coherent radiation may be obtained using laser-produced plasmas. There are no fundamental limitations here; it only remains to find the optimal conditions for producing a plasma plume to serve as the nonlinear medium for HHG. Laser-produced plasma may be validly used for this process if the effect of the limiting factors (self-defocusing and the wave phase mismatch of the harmonics and the radiation being converted) is minimized [17, 20, 22]. The authors of Ref. [17] noted that the plasma produced on the surface of a target should be an efficient medium for HHG, whatever the target material is. Anticipating things, we note that recent HHG research has exhibited the decisive effect of physical target parameters on the properties of the frequency conversion of laser radiation.

Among the special features of HHG in laser-produced plasmas, we first of all note the wide range of nonlinear medium characteristics available for varying the conditions of laser plume production on the surface of a solid. This applies to plasma parameters such as the plasma dimension, the density of ions, electrons, and neutral particles, and the degree of their excitation. The use of any elements of the periodic table that exist as solids largely extends the range of materials employed, whereas only four light rare gases are typically used in gas-jet HHG schemes. In several cases, this furnishes an opportunity to realize quasiresonance conditions for a sharp increase in the efficiency of single harmonic generation due to the effect of ion transitions on the nonlinear response in the spectral range in question. This effect can hardly be realized in gas-jet HHG schemes because of a low probability that the atomic transition frequencies of the gases coincide with the frequencies of single harmonics.

The advantages of in-plasma HHG could largely be realized with the use of a low-excited and weakly ionized plasma, because the limiting processes governing the dynamics of laser frequency conversion would play a minor role in this case. Attention was drawn to this feature early in the study of third harmonic generation in a weakly ionized plasma (see review [24]). An analysis of low-order (third [25, 26] and fifth [27]) harmonic generation in such plasmas produced by a laser prepulse on the surface of a solid target allowed formulating several recommendations as regards further advancement toward shorter wavelengths. It is significant that the use of femtosecond pulses enabled producing low-order harmonics with a relatively high conversion efficiency (of the order of 10^{-3} in the case of the third harmonic from the plasma produced in optical breakdown in air [28, 29]).

This assumption was confirmed by several recent papers concerned with high-order harmonic generation in the plasma medium [30 – 34]. A substantial increase in the highest order of the generated harmonics, the emergence of a plateau in the energy distribution of highest-order harmonics, the high efficiencies obtained with several plasma formations, the realization of resonance enhancement of individual harmonics, efficient harmonic enhancement for plasma plumes containing clusters of different materials, and other properties revealed in these and other works [35 – 38] have demonstrated the advantages of using specially prepared plasmas for HHG.

The orders of harmonics obtained in plasma media to date range into the sixties and seventies [30, 32, 39, 40]. The highest-order harmonics (the 101st harmonic, $\lambda = 7.9$ nm) have been obtained in manganese plasmas [41]. The efficiency of conversion in the plateau region amounts to $\sim 10^{-5}$ [42]. In addition to that, the efficiency of conversion to an individual (resonantly enhanced) high-order harmonic approaches 10^{-4} [31, 32]. The majority of these parameters are at the same level as the results obtained in gas media. But the highest orders of harmonics produced by these two techniques remain radically different. For gases, the generation of harmonics of orders exceeding 2000 has been reported [43]. The substantial difference in the orders of harmonics generated in gases and in plasmas raises the problem of searching for new ways to produce higher-energy coherent photons by means of HHG in plasma plumes. In Section 5, in the example of the plasma produced on the surface of manganese and vanadium, we show that this opportunity is provided by doubly charged ions, which increase the maximum attainable energy of the coherent short-wavelength photons generated.

Another problem involves the quest for new plasma media that would favor the enhancement of an individual harmonic. The production of a single high-intensity harmonic (rather than a group of harmonics of equal intensity in the plateau region) would open up the way to the practical application of these coherent short-wavelength radiation sources. Because resonantly enhanced harmonics have already been observed in several plasma media, there are strong grounds to believe that similar conditions will be discovered for other plasma formations. The generated harmonic frequency may then be tuned to transitions with a high oscillator strength by

frequency tuning of the laser system [31, 37, 38], as well as by varying the chirp of the laser radiation [32, 34, 36].

The theoretical foundations of HHG in an isotropic medium are set out at length in works relating to the early stages of HHG research [23, 44, 45] and in recent papers [46–49]. We do not consider HHG in gas jets under the conditions of plasma effects occurring due to ionization by femtosecond pulses, because this topic has been covered by recent comprehensive papers (see, e.g., Refs [3, 4, 50, 51]). Nor do we consider the mechanisms of odd and even harmonic generation in the reflection of laser radiation from surfaces, because this problem is discussed at length in several reviews and papers [2, 8, 52, 53] and, furthermore, is beyond the scope of our paper. Because our aim in this paper is to familiarize the reader with new approaches to harmonic generation in the XUV range with the use of an isotropic medium (different from that used previously in gas-jet sources and special gas-filled cells), we primarily discuss the experimental results obtained in this area. We note that several results under discussion were considered in a previously published brief review of HHG in plasma [54]. In the present paper, we give a more comprehensive picture of the processes observed in HHG in plasma plumes and consider new techniques that have emerged only recently. Among them are the use of nanoparticles as components of laser-produced plasmas, numerical analysis of resonance harmonic enhancement, and complex targets for plasma production.

We outline the findings of investigations into the efficient generation of short-wavelength XUV radiation in the propagation of femtosecond laser pulses through a low-excited plasma produced on the surface of different solid-state targets. The structure of the paper is as follows. In Section 2, we outline the basic ideas of high-order harmonic generation and the experimental schemes used for HHG in plasmas. Research on the resonance enhancement of individual harmonics observed in different plasmas is presented in Section 3. The generation of harmonics of the doubled frequency of titanium–sapphire laser radiation is discussed in Section 4. The properties of HHG in various weakly ionized plasma structures are considered in Section 5. Section 6 is concerned with the analysis of the application of different laser pulses (with durations varying over five orders of magnitude) for producing optimal plasmas for HHG. In Section 7, the plasma characteristics are analyzed from the standpoint of optimization of the frequency conversion of laser radiation. The application of nanoparticle-bearing plasmas for improving the HHG efficiency is discussed in Section 8. Investigations into HHG in laser-produced plasmas are summarized in Section 9.

2. Fundamentals of high-order harmonic generation in isotropic media

The high-order harmonics of laser radiation may be generated by three different techniques: (i) in the interaction of laser pulses (radiation intensity $I \sim 10^{14}-10^{16}$ W cm^{-2}) with gas jets or a specially prepared gas located in cells and waveguides; (ii) in the interaction of laser pulses with a higher intensity ($I > 10^{17}$ W cm^{-2}) and a high contrast ratio (10^6 and higher) with the surfaces of solids; and (iii) in the passage of laser radiation ($I \sim 10^{14}-10^{15}$ W cm^{-2}) through specially prepared (using prepulses) plasma media. We do not consider the second technique here. Investigations of HHG from surfaces are analyzed in detail in monograph [55] and review [56]. We only briefly touch upon the problems arising in HHG in gas jets. These processes are analyzed in monograph [57]. HHG in gases is also investigated in comprehensive reviews [58, 59]. Our main concern is with the analysis of HHG in the passage of moderately intense radiation through laser-produced plasmas, i.e., the plasmas produced on the surfaces of different solid targets using additional subnanosecond laser pulses timed with the main femtosecond laser pulse (under conversion).

When a high-intensity laser pulse passes through a gaseous or plasma medium, its atoms and ions emit odd harmonics. For a laser radiation wavelength λ, a superposition of the components λ, $\lambda/3$, $\lambda/5$, $\lambda/7$, etc. is observed at the output of the nonlinear medium. The harmonics of laser radiation result from a three-stage process [23, 44, 45] that comprises the ionization of an atom (or ion), the electron acceleration in the electromagnetic field, and the subsequent recombination (with an ion) and emission of harmonics (Fig. 1). This process is periodically repeated every half cycle of the electromagnetic wave. The highest-order harmonics are due to the electron acceleration at the instant of ionization at the peak intensity of the laser pulse. Therefore, the generation of highest-order harmonics results from the interaction of a high-intensity light field with atoms [60–62], atomic clusters [63, 64], molecules [65, 66], and ions [17, 19, 20, 24, 67–75].

A characteristic feature of the three-stage HHG is a rapid decrease in the intensity of first (low-order) harmonics followed by a long plateau where the intensities of high-order harmonics differ only slightly from one another, and an abrupt decrease in the intensity of the highest-order harmonics generated (the so-called harmonic cutoff H_c). The position of H_c is determined by the ionization potential I_i of the particles participating in harmonic generation (of atoms in the case of HHG in gases and of ions in the case of HHG in a plasma) and by the ponderomotive potential, which defines the accelerated electron energy and depends on the intensity of femtosecond radiation and it wavelength ($U_p \approx 9.3\times10^{-14} I_{fp}$ [W cm^{-2}] λ^2 [μm^2]). The highest photon energy of the harmonics generated is defined by the relation $E_c \approx I_i + 3.17U_p$.

The main HHG properties may be characterized with the aid of a semiclassical model [23, 44, 45], although a more accurate description calls for a consistent quantum mechanical treatment. In the semiclassical model, an electron detached from an atom is considered a free particle, and the effect of all bound states, with the exception of the ground state, is assumed to be negligible. These assumptions are satisfied in the tunnel ionization regime, which is characterized by the inequality $\gamma < 1$ for the Keldysh parameter

$$\gamma = \omega_L (2I_i)^{0.5} E^{-1}, \quad (1)$$

where ω_L is the laser radiation frequency and E is the magnitude of the electric vector of the electromagnetic wave. High-power ultrashort laser pulses are best suited for the fulfillment of these conditions.

Along with the microscopic consideration of the processes occurring in the interaction of high-power ultrashort laser pulses with atoms and ions, account should also be taken of macroscopic processes such as the effect of transmission through a medium and group effects. These effects primarily include dephasing, absorption, and defocusing. These processes are analyzed in Ref. [46].

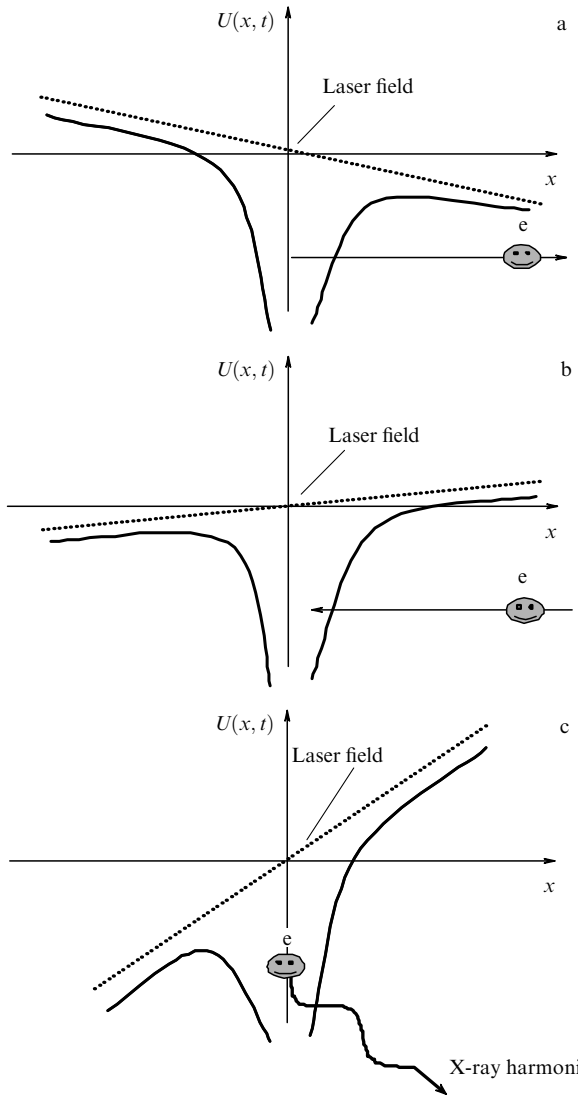

Figure 1. Three-stage mechanism of high-order harmonic generation: (a) tunnel ionization, (b) electron acceleration in the electromagnetic field of the laser wave, (c) recombination with the ion and the emission of harmonics.

Below, we consider the experimental setups used for HHG in plasma media. Figure 2 gives one of these experimental setups [30]. The femtosecond pulses of laser radiation with a wavelength λ are focused into the plasma plume produced on the surface of a solid-state target with the aid of a laser prepulse several hundred picoseconds long. The harmonics at the wavelengths $\lambda/(2n-1)$ are generated in the laser-produced plasma in the direction of the femtosecond pulse propagation and are spatially separated with a diffraction grating. The harmonic intensities are measured with a high-energy photon detector.

The majority of investigations into HHG in laser-produced plasmas were conducted by three scientific groups (the Institute for Solid State Physics, Japan; the Centre for Advanced Technology, India; and the Institut National de la Recherche Scientifique, Canada) with the use of commercial titanium–sapphire lasers operating in the chirped-pulse amplification mode [31, 32, 67]. A fraction of the uncompressed subnanosecond radiation (pulse duration $t = 210-300$ ps, pulse energy $E = 5-30$ mJ, wavelength $\lambda = 790-800$ nm, pulse repetition rate 10 Hz) was used as a

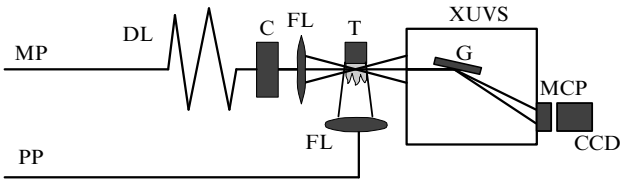

Figure 2. Example of experimental setup for high-order harmonic generation in a laser-produced plume: MP, main pulse; PP, prepulse; DL, delay line; C, compressor; FL, focusing lenses; T, target; XUVS, XUV spectrometer; G, diffraction grating; MCP, microchannel plate; CCD, charge-coupled device.

prepulse to produce a plasma on the target surface (see Fig. 2). The prepulse radiation was focused onto a spot measuring several hundred micrometers on the target surface. The prepulse intensity at the target surface varied in the range $I_{pp} \sim 5 \times 10^9 - 9 \times 10^{10}$ W cm^{-2}. The plasma produced under these conditions consisted primarily of neutral particles and singly charged ions. The main femtosecond laser pulse ($t = 35-150$ fs, $E = 10-100$ mJ, $\lambda = 790-800$ nm, spectral pulse width 12 – 38 nm) was focused into the plasma with a delay varied between 10 and 150 ns.

The peak femtosecond radiation intensity in the focal region amounted to $I_{fp} = 4 \times 10^{17}$ W cm^{-2}. This intensity far exceeded the tunnel ionization intensity for singly charged ions, resulting in a violation of the optimal HHG conditions due to the production of a large number of free electrons. That is why the focal point was positioned upstream or downstream of the plasma plume such that the in-plasma intensity fell in the range 2×10^{14} W cm^{-2} to 5×10^{15} W cm^{-2}. High-order harmonics were analyzed by means of an X-ray spectrometer with a grazing-incidence grating (Hitachi, 1200 grooves/mm). Extreme ultraviolet spectra were recorded with a microchannel plate and a CCD camera. The spectral characteristics of the laser-produced plasma in the visible and near-ultraviolet ranges were analyzed with a USB2000 spectrometer. The absolute laser-to-harmonic radiation conversion efficiency was measured by comparing the efficiencies of the third harmonic generation in crystals and in the plasma, with the subsequent comparison of the intensities of higher-order harmonics. This calibration is described in detail in the example of harmonic generation in silver plasmas [42].

3. Resonance enhancement of individual harmonics

As already noted in the Introduction, the possibilities for using harmonic radiation are limited due to a low conversion efficiency during HHG. Several techniques have been elaborated to improve the conversion efficiency when using gas jets as the nonlinear medium for HHG. One of these techniques involves phase matching of harmonic waves and the fundamental wave with the help of variable-width gas-filled waveguides [7]. Forming resonance conditions to enhance the nonlinear optical response of the medium may be an alternative to this technique. The role of atomic resonances in increasing the laser radiation conversion efficiency was actively discussed in the framework of the perturbation theory at the early stages of the study of low-order harmonic generation (see monograph [76] and the references therein). In the case of HHG, the increase in the

efficiency of generated harmonics due to resonance processes has come under discussion relatively recently, and this approach appears to have considerable promise with the use of ion and, in some cases, atomic resonances [14, 16, 77 – 80]. The papers cited above comprise both the theoretical treatment of the process and the description of the first attempts to form resonance conditions in experiments. While theoretical estimates testified to the possibility of an efficient enhancement of individual harmonics and groups of harmonics, experimental works revealed the difficulties encountered in HHG in gases.

Therefore, the use of plasma media could largely facilitate the solution to the problem of resonance harmonic enhancement. Examining a large group of potential targets allowed identifying some of them as suited for demonstrating this process [34]. The advantages of 'plasma HHG' over 'gas HHG' were amply manifested in this case, because the number of possible media in the former case is far greater than in the latter case.

Originally, the resonance conditions in HHG in a plasma were attained by frequency tuning of the laser system oscillator to the resonance transition frequency that might be responsible for increasing the nonlinear optical response of the medium at the wavelength of one individual harmonic or another [31, 37, 38]. We note that this technique has several disadvantages. In particular, tuning the oscillator spectrum in a complex laser facility cannot directly lead to the corresponding change in the spectrum of output laser pulses (because of the narrowing of the amplification spectrum resulting from the shift of the wavelength from the 'optimal' value characteristic of the laser system). Account should also be taken of the amplification saturation at the central wavelength, which necessitates a realignment of the system on shifting the oscillator spectrum. Furthermore, this necessitates a realignment of the stretcher and compressor, and hence the spectrum tuning of the entire laser system with the other output parameters (the energy, duration, and spectral width of the laser pulse) kept unchanged turns out to be a nontrivial problem. A much simpler method of spectral tuning of harmonic frequencies (without tuning the spectrum of the laser system) may be realized by chirping the laser radiation [81]. The harmonic wavelength shifts to the long-wavelength side of the spectrum for a positive chirp of the pulse under conversion, with the leading edge of the pulse primarily containing the long-wavelength components of the laser radiation spectrum. The same is true of harmonics shifted to the short-wavelength side of the spectrum in the case of negatively chirped pulses. This technique is comprehensively described in Refs [34, 81].

3.1 Enhancement of the 13th harmonic in an indium plasma

A typical harmonic spectrum generated in indium plasmas using 150-fs-long pulses with the wavelength 796 nm is shown in Fig. 3. Harmonics up to the 39th order ($\lambda = 20.4$ nm) were observed in these experiments. The high-order harmonic intensity distribution was plateau-like in shape, i.e., the intensities of adjacent harmonics were only slightly different up to the point of the highest generated order, when the intensities of harmonics with the highest photon energy decreased dramatically (see Fig. 3, curve *1*). Also shown for comparison is the harmonic distribution obtained in silver plasmas (see Fig. 3, curve *2*). In the case of indium plasma, the efficiency of conversion to the harmonics was equal to

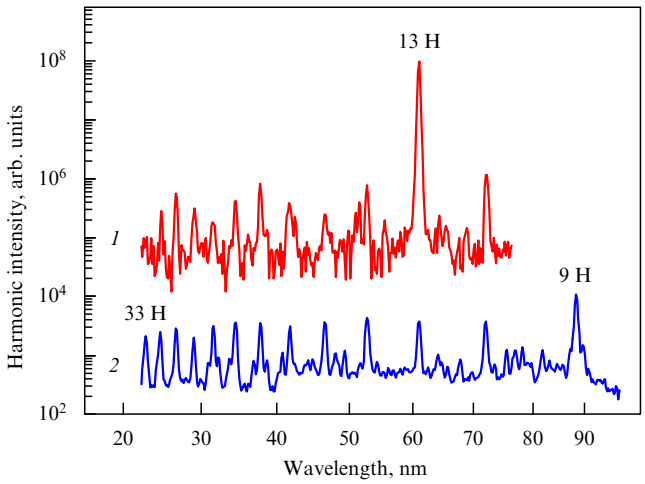

Figure 3. High-order harmonic spectra generated in indium (*1*) and silver (*2*) plasmas.

1×10^{-6} in the plateau region. This spectrum shows that the 13th harmonic intensity is much higher than the intensities of the neighboring harmonics. The efficiency of conversion to the 13th harmonic was equal to 8×10^{-5}, which corresponds to 0.8 μJ for a femtosecond pulse energy of 10 mJ [31]. An even higher efficiency (10^{-4}) of conversion to this harmonic was recorded with the use of shorter pulses with a higher energy (48 fs, 25 mJ). In this case, the 13th harmonic intensity was 200 times the intensity of the neighboring harmonic [32, 75].

The observation of so substantial an excess of the individual harmonic intensity over all the rest raises the question of whether the radiation attributed to the 13th harmonic ($\lambda = 61.2$ nm) was an amplified spontaneous emission, a result of plasma overexcitation caused by the passage of the femtosecond pulse, or a result of the process caused by the strengthening of the nonlinear optical plasma-plume response at the wavelength of this individual harmonic due to a quasiresonance with ion transitions having high oscillator strengths.

First, to verify that the 61 nm radiation arises not from the reradiation of a plasma line but from a nonlinear process, the effect of femtosecond radiation polarization on the intensity of this line was investigated. A quarter-wave plate was placed in front of a focusing lens to change the polarization of radiation interacting with the plasma. Minor deviations from the linear polarization resulted in a substantial lowering of the 61.2 nm radiation intensity, as well as of the other generated harmonics, which is typical for HHG in an isotropic medium. The use of circularly polarized radiation had the effect that the harmonics vanished completely, while the plasma radiation spectrum remained unaltered.

Second, the femtosecond source wavelength was tuned in order to determine whether the coincidence of an indium plasma line with the laser harmonic frequency was the reason why the individual harmonic intensity was so much higher than the other harmonics. The central wavelength of a titanium–sapphire laser was tuned in the wavelength range from 770 to 796 nm. The 13th harmonic intensity became substantially lower on tuning the wavelength from 796 nm to shorter wavelengths. At the same time, the intensity of the 15th harmonic at the wavelength 782 nm was observed to increase significantly, while the intensities of other harmonics

did not undergo appreciable change. These experiments demonstrated the effect of indium ion transitions on the intensities of individual harmonics.

These investigations bring up the question: why did the intensity of an individual harmonic so much exceed the others in the case of indium plasma? Earlier investigations of indium plasmas showed that the bulk of emission in the 40 – 65 nm wavelength range was due to radiative transitions to the ground state $4d^{10}\,5s^2\,{}^1S_0$ and the low-lying excited state $4d^{10}\,5s\,5p$ [82]. These investigations also revealed a strong 62.1 nm line (19.92 eV) corresponding to the transition $4d^{10}\,5s^2\,{}^1S_0 \rightarrow 4d^9\,5s^2\,5p\,(^2D)\,{}^1P_1$. The oscillator strength of this transition was equal to 1.11, which exceeded the corresponding parameters of other transitions in this range by more than a factor of 12. This transition may be tuned to resonance with the 13th harmonic ($\lambda = 61.2$ nm, $E_{ph} = 20.26$ eV) due to the Stark effect.

3.2 Enhancement of individual harmonics in Cr, GaAs, Sb, Sn, Mn, and InSb laser-produced plasmas

The selection of these targets was preceded by an analysis of HHG in different media, which showed the feasibility of obtaining resonantly enhanced harmonics in some of them. For the majority of plasmas produced in different targets, the harmonic intensity distribution was plateau-like in shape, with a different degree of intensity lowering of each successive XUV harmonic. The targets specified above were investigated in greater detail, because in these cases it was possible to observe an enhancement of one harmonic or another of titanium–sapphire laser radiation (48 fs, 795 nm) in different plateau regions. The radiation spectra converted using these targets were compared with the harmonic spectrum obtained using indium plasma.

Higher harmonics of the orders up to 29 (27.3 nm), 43 (18.4 nm), and 47 (16.9 nm) were observed in InSb, GaAs, and Cr plasmas. In these investigations, nonchirped 48-fs-long pulses were used. Under the specified conditions, these plasma media exhibited some enhancement (and in some cases, depression) of individual harmonics. In subsequent experiments, the chirp of laser radiation was varied by varying the separation of compressor gratings in the laser system. Varying the laser pulse chirp entailed a significant redistribution of the enhanced harmonic intensities in the spectrum, while the unenhanced harmonics were hardly changed. The aim of these investigations was to demonstrate the feasibility of enhancing an individual harmonic, not only at the beginning of the plateau (as for an indium plasma) but also in the middle and even at the end of the plateau.

In the generation of harmonics in Cr plasma, the intensity of the 27th harmonic exhibited significant variations under variation of the laser radiation chirp [34, 83]. In this case, the intensity ratio between the 27th harmonic and the neighboring harmonics in the chromium plasma spectrum varied from 0 to 1. At the same time, the 29th harmonic ($\lambda = 27.3$ nm) far exceeded the neighboring harmonics in the central part of the plateau (Fig. 4). The enhancement of this harmonic was observed in nonchirped laser pulses. Variations of the radiation chirp led to variations in the intensity of this harmonic, as for the 27th harmonic. The ratio of the intensities for the 29th and 31st harmonics was equal to 23. We note that the spectral harmonic widths were narrower in negatively chirped pulses. As is evident from Fig. 4, for a strong chirp, the harmonic spectrum deviated strongly from the spectrum generated under conditions that ensured substantial variations of the intensities of the 27th and 29th harmonics.

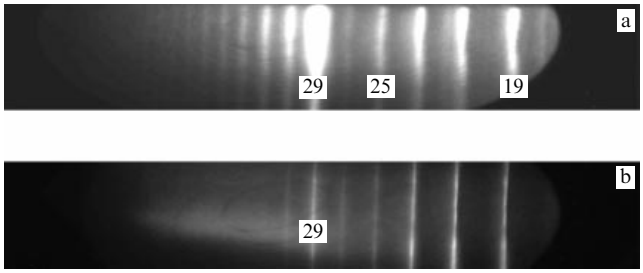

Figure 4. Distribution of harmonics obtained in chromium plasmas in the case of nonchirped 48-femtosecond pulses (a) and negatively chirped 160-femtosecond pulses (b).

Similar variations in the harmonic intensity distribution were observed in the plasmas of several semiconductors (GaAs, InSb). For nonchirped pulses and for negatively chirped radiation, the harmonics generated in the plasma of gallium arsenide exhibited a plateau-like intensity distribution with a minor harmonic intensity lowering for each successive order. However, the picture was significantly different for positively chirped pulses: the 27th harmonic ($\lambda = 29.4$ nm) had a high intensity. The intensity of this harmonic, which was located at the end of the plateau-like distribution, was six times higher than the neighboring harmonic intensities [36]. We note that the efficiency of conversion to the harmonic in this case was largely dependent on the focal plane position of the lens relative to the laser plume region. The laser radiation-to-harmonics conversion efficiency was highest when the focal point was either behind or in front of the laser plume, depending of the specific experimental conditions [84].

In an InSb plasma, a substantial enhancement of the 21st harmonic ($\lambda = 37.8$ nm) was observed when using nonchirped laser pulses (Fig. 5). The intensity of this harmonic exceeded the neighboring-order harmonic intensities by a factor of 20 [32]. In this plasma, as in the previous cases, the high-intensity harmonic underwent substantial changes under chirp variations. In particular, the enhancement factor for the 21st harmonic was equal to 10 with the use of positively chirped 140-fs-long pulses. For negatively chirped pulses, the enhancement factor for this harmonic was much smaller.

To determine the enhancement mechanism for radiation near the wavelengths 27.3 nm (for the 29th harmonic generated in a Cr plasma), 29.4 nm (for the 27th harmonic in a GaAs plasma), and 37.8 nm (for the 21st harmonic in an InSb plasma), the effect of differently polarized laser radiation was analyzed (as with the indium plasma). It was shown that the radiation at the above wavelengths vanished when circularly polarized radiation was used, which could be expected considering the nonlinear optical nature of the spectra observed.

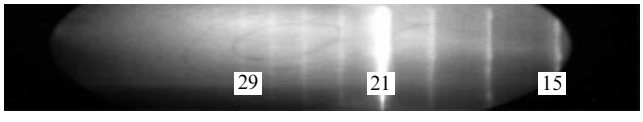

Figure 5. Distribution of the harmonics of nonchirped 48-femtosecond pulses obtained from an InSb plasma.

The XUV spectrum of antimony plasma is dominated by two peaks of Sb I: one of them is broad (1 eV) and lies in the 31.24 eV region, and the other is narrow (0.2 eV) and lies in the 32.22 eV region [85]. The emission spectrum of the low-excited plasma also contains a considerable number of Sb II lines, which increase the emission intensity in the 32.4–32.7 eV range. However, the highest value of gf among the transitions of ions and neutral atoms of Sb is in the transition $4d^{10}5s^25p^3\,{}^2D_{5/2}-4d^95s^25p^4({}^3P)^2F_{7/2}$ ($E\approx 31.5$ eV, gf = 1.54). This gf value is several times higher than other values of this parameter in the specified spectral range. At the same time, among the gf values calculated for $4d^{10}5s^25p^2-4d^95s^25p^3$ Sb II ion transitions, the value of this parameter for the transition ${}^3P_2-({}^2D)^3D_3$ ($E\approx 32.8$ eV) is also rather high, which may to a certain degree affect the nonlinear optical plasma response due to the proximity of the harmonic wavelength to the wavelength of this transition. In particular, the 21st harmonic (37.8 nm, $E_{ph}\approx 32.9$ eV) of the laser used may be tuned to these transitions by varying the laser radiation chirp, as well as by using the Stark shift in the intense wave field, which should increase the intensity of this harmonic. This effect was observed in experiments involving radiation with various durations and chirps. The strongest enhancement of this harmonic was obtained for positively chirped 210-fs-long pulses [86].

Observed in tin plasmas was an enhancement of the 17th harmonic (47.1 nm, 26.5 eV). As in the previous cases, the chirp variations of converted laser pulses led to substantial variations in the intensity of this harmonic relative to the neighboring harmonic intensities (Fig. 6) due to variations in the harmonic wavelength and the corresponding tuning to the resonance transitions of Sn ions. For this harmonic, the greatest enhancement factor (15) was obtained for negatively chirped 70-fs-long pulses. A similar effect of the 17th harmonic enhancement (by a factor of 20) in tin plasmas was studied in Ref. [37], where the harmonic was tuned to the Sn ion transition with a high oscillator strength by means of tuning the laser system oscillator. An analysis of Sn II photoabsorption spectra revealed the existence of a strong transition $(4d^{10}5s^25p^2P_{3/2}-4d^95s^25p^2({}^1D)\,{}^2D_{5/2})$ at the wavelength 47.20 nm ($E_{ph}=26.24$ eV) [87, 88]; its parameter gf = 1.52 was more than five-fold greater than for other transitions from the ground state of singly charged tin ions. This transition was supposedly responsible for the enhancement of the 17th harmonic in the tuning of its wavelength [86].

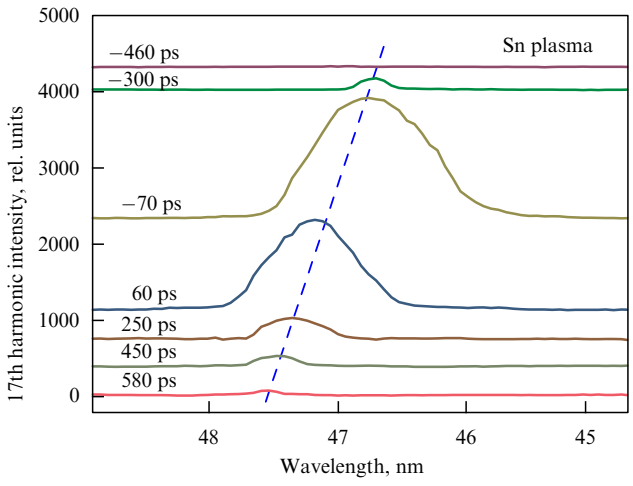

Figure 6. Intensity and spectrum variations of the enhanced 17th harmonic generated in Sn plasma for different chirps and durations of laser pulses.

Two-component targets were also investigated along with the single-component specimens mentioned above [89–92]. Simultaneous excitation of chromium and tellurium resulted in the enhancement of the 27th and 29th harmonics in this plasma plume. These investigations showed that the nonlinear processes occurring in different plasma components were independent.

The virtually total absence of reports about resonance enhancement of the generation efficiency for individual harmonics in laser radiation conversion experiments in gas jets may be explained based on a comparison of the atom and ion excitation spectra recorded from the plasmas of solid-state targets and gas jets. In the latter case, 4–5 gases are normally used, and the probability of attaining optimal resonance conditions is much lower than that for numerous solid-state targets. However, even with solid-state targets, it has so far been possible to discover only a few specimens wherein the conditions for individual harmonic enhancement are realized.

3.3 Analysis of the results of investigations into enhanced-harmonic generation in the plasmas of several targets

The main difference between the experimental data on resonance harmonic enhancement and the results of the theory in Ref. [15] is that the theory predicts the resonance enhancement, under specific conditions, not of an individual harmonic but of a group of harmonics. In the cases described in Sections 3.1 and 3.2, as well as in similar papers concerned with resonance harmonic enhancement [31, 32, 34, 38, 86], the enhancement of only one harmonic was observed. Meanwhile, these investigations demonstrated the enhancement of a group of harmonics [from the 33rd to the 41st (see Section 5.4)] in the conversion of laser radiation in manganese plasmas, which is possibly the first experimental verification of the theory of resonance enhancement elaborated in Ref. [15].

The theoretical postulates are underlain by the idea of free-electron dynamics. Electrons may have a nonzero initial velocity when they are 'extracted' from atoms via tunnel ionization from excited levels. As a result of acceleration in the electromagnetic wave field and elastic collisions with the parent ion, an electron may subsequently experience elastic collisions twice during each wave oscillation cycle. The theory predicts that the occurrence of a multiphoton resonance with transitions having large gf values, as well as the Stark effect, may result in a resonant enhancement of harmonics with the energy $\hbar\omega_n$ satisfying the relation

$$1.4U_p + I_{pn} \leqslant \hbar\omega_n \leqslant 2U_p + I_{pn}\,, \qquad (2)$$

where I_{pn} is the ionization potential of the nth excited bound state ($n = 0$ corresponds to the ground state) to which the electron recombines.

Using the optimal intensity obtained in the experiments with manganese plasmas ($I_{fp} = = 4\times 10^{14}$ W cm^{-2}) and the second ionization potential of Mn (15.6 eV) in relation (2), we infer that a group of harmonics of the orders from 33 to 41 may be enhanced in the conversion of radiation with the wavelength 800 nm, and that only a single (the 17th) harmonic may be enhanced in the case of 400 nm radiation.

These estimates were confirmed both by the investigations under review (see Section 5.4) and by experiments involving the second harmonic of 800 nm radiation, which demonstrated the enhancement of the 17th harmonic in a manganese plasma (see Section 4). We note that manganese has strong resonance transitions in the wavelength range corresponding to the titanium–sapphire laser radiation ($\sim$ 800 nm) harmonics of the orders from 33 to 41.

If follows from the experimental data outlined above that the enhancement of an individual harmonic in the plateau region is underlain by an increase in the HHG efficiency under the resonance strengthening of the nonlinear response of a laser-produced plasma. That is why this mechanism is analyzed in greater detail below. We emphasize that the study of the role of atomic and ion resonances in harmonic generation was one of the principal goals at early stages of research into the generation of harmonics of relatively low orders, and the effect of atomic and ion resonances was adequately described by the perturbation theory [76, 93]. In recent investigations [15], the enhancement of harmonics was related to the occurrence of the oscillating trajectories of electrons that interact with the ion during the accelerated electron tunneling from the atom or ion. An increase in individual harmonic intensities may also be considered in the framework of the resonance enhancement model based on the one-dimensional time-dependent Schrödinger equation for simple model potentials [14]. However, as noted above, this model implies—along with an enhancement of the 'resonance' harmonic—an enhancement of a group of higher-order harmonics [77], which is at variance with experimental observations: only the harmonic that was at resonance with excited atomic and ion states was enhanced.

The enhancement of a single (the 13th) harmonic for electrons with a nonzero initial energy was considered and demonstrated [15] for specific conditions. Estimates suggest that a similar enhancement of the 13th harmonic may be observable at the laser radiation intensities 1.2×10^{14} W cm^{-2} and 2.3×10^{14} W cm^{-2} with the inclusion of the effects of In I and In II, respectively. The findings in Ref. [15] imply that the intensity enhancement of an individual harmonic should appreciably depend on the wavelength and intensity of laser radiation. Meanwhile, an increase in the individual harmonic intensity arising from resonance processes was experimentally observed in a wide range of laser radiation intensities. This fact is indicative of the possibility for the adjustment of resonance enhancement occurring during the laser pulse action. To interpret the observed features, a detailed analysis should be performed to include the effect of inner-shell electrons (along with the effect of outer-shell electrons).

Such an enhancement of an individual harmonic may be due to electron trajectories such that the electron approaches the parent ion and interacts with it twice per cycle of the laser wave [15]. Because these electron trajectories originate in a resonantly populated excited state and have a nonzero kinetic energy, the electrons accordingly have a nonzero energy in approaching the ion. As the three-level model suggests, recombination is responsible for the emission of harmonics. Because of the low probability of this process, however, the density of electrons accelerated by the laser field increases, as does the probability of reradiating the excess electron energy in the form of harmonic radiation with an increase in the number of electron–ion collisions. These multiple collisions are responsible for the intensity increase of those harmonics that are close to atomic or ion resonances.

Several experimental observations (like the dependence of harmonic intensities on the position of laser focal point, the size of the plasma region, and the radiation intensity) suggest that these features arise from the collective nature of HHG. An analysis of the phase relations between the laser and harmonic radiation waves should comprise studies of the effect of spatial and temporal nonuniformity of the radiation to be converted. Among the factors responsible for the enhancement of individual harmonics, we note the difference between the phase matching conditions for different harmonics. The phase mismatch ($\Delta k = nk_{\rm laser} - k_i$, where k_i is the ith harmonic wavenumber) varies as a laser pulse passes through a plasma plume due to the attendant further ionization of the nonlinear medium. According to theoretical estimates assuming equal densities of the plasma particles, the phase mismatch due to free electrons for harmonics in the plateau region is one to two orders of magnitude larger than the mismatch due to atoms and singly charged ions. Under resonance conditions, when the frequency of some harmonic becomes close to the frequency of inner-shell atomic transitions, the wavenumber variations for this harmonic caused by the atoms may be significant and the free-electron effect may be canceled. In these circumstances, it is possible to satisfy the optimal phase relations for one harmonic, with a consequential increase in the conversion efficiency for only this harmonic.

Analyzing the enhancement of individual harmonics is important for understanding the processes that affect the nonlinear optical response of plasma plumes. Here, we briefly outline the theoretical model of resonance HHG [46, 47] as applied to Sb II, Cr II, and Te II ions [92]. The generation of enhanced harmonics in these ion media was reported in Refs [34, 38, 72, 83, 86]. We note that the resonance harmonic enhancement was also analyzed for complex targets: diatomic molecules [90] and two-component targets [92]. The theoretical model implies that owing to significant absorption on certain transitions of these ions, the population of excited metastable states increases under the action of the excitation energy $\Delta\omega = E_2 - E_1$. Produced in this case is a coherent superposition of the ground state (with the energy E_1) and the excited state (with the energy E_2). When the wavelength of linearly polarized radiation is at resonance with this transition, the radiation of harmonics at the frequencies $\Omega = \Delta\omega \pm 2n\omega = (2n_{\rm R} + 1 \pm 2n)\,\omega$, $n = 0, 1, 2, \ldots$ is possible, along with the radiation of conventional harmonics at the frequency $(2k + 1)\,\omega$.

The first numerical results for tin ions [46, 47], which show an appreciable enhancement of the 17th harmonic, are in satisfactory qualitative agreement with experimental data [37]. Other harmonics form a plateau followed by a sharp decrease in harmonic intensities, in accordance with the three-stage HHG model [23, 44, 45]. In the theoretical model describing resonantly enhanced harmonics, the neighboring (the 15th and 17th) harmonics are also somewhat enhanced. A possible explanation of this discordance with the data of experiments [in which no enhancement of the neighboring harmonics was observed, as in all other cases with enhanced harmonics (see Section 3.2)], is that this theoretical model relies on the strong-field approximation, which may not be sufficiently correct for low-order near-resonance processes and does not include Coulomb effects. The data obtained show that the harmonic radiation (or the fundamental laser

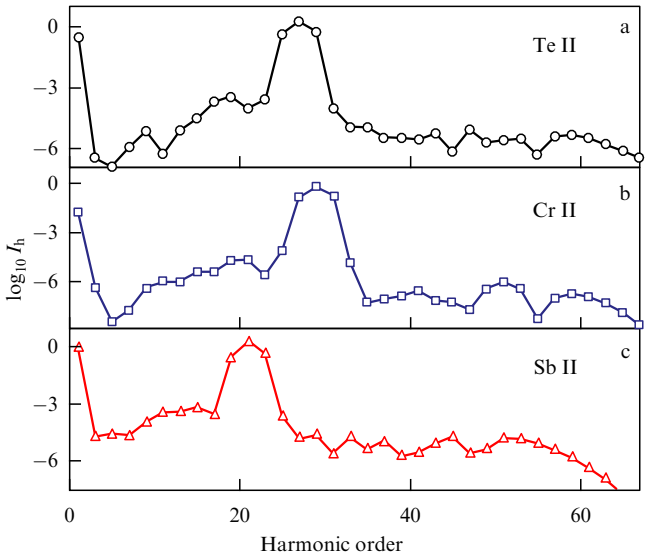

Figure 7. The harmonic intensity (I_h) distribution calculated for HHG in Te II (a), Cr II (b), and Sb II (c).

wave) should not necessarily be exactly tuned to resonance for observing harmonic enhancement. Considering the qualitative agreement between the proposed model and experiments for Sn II, it would be expedient to compare its findings with other experimental data on resonance enhancement, in particular, for Sb II, Cr II, and Te II ions.

Figure 7 shows the data of numerical calculations for HHG in these plasma media for the fundamental radiation wavelengths used in experiments. We can see that the 21st harmonic is enhanced in Sb II (Fig. 7c, $E_1 = -16.63$ eV, $\Delta\omega = 32.79$ eV), which is in qualitative agreement with experimental data [38]. The 29th harmonic is enhanced in the case of chromium ions (Fig. 7b, $E_1 = -16.48$ eV, $\Delta\omega = 45.23$ eV), which is consistent with the data in Ref. [83]. Lastly, theoretical calculations suggest an enhancement of the 27th harmonic in tellurium plasmas (Fig. 7a, $E_1 = -18.6$ eV, $\Delta\omega = 40.18$ eV), which is also in qualitative agreement with experimental data [72]. The three calculated spectral harmonic intensity distributions terminate with an abrupt intensity decrease in the highest harmonics. Some enhancement of the harmonics nearest to the most-enhanced one may be explained along similar lines as for the HHG calculations for tin plasmas outlined above. The authors of Ref. [92] point out that a theoretical description of the resonance enhancement of individual harmonics that would be in perfect agreement with experimental data, and with the enhancement of an individual harmonic in particular, has yet to be given.

4. Generation of the harmonics of 400 nm radiation propagating through a laser-produced plasma

In the conversion of laser radiation to the XUV range, high-intensity short-wavelength sources offer several advantages over the conventional source (a titanium–sapphire laser) used in the majority of experiments. In particular, the effect of free electrons on the phase matching of HHG is weakened when using shorter-wavelength radiation. At the same time, according to the three-stage model describing HHG in gases and in plasmas, the highest generated photon energy (E_c) should decrease with decreasing the wavelength proportionally to λ^2. Accordingly, the highest generated harmonic order must vary with the wavelength in proportion to λ^3.

The first observations of HHG with the use of short-wavelength lasers (a KrF excimer laser, $\lambda = 248$ nm) were reported in Refs [17, 18]. Harmonics up to the 21st order were observed in lead plasmas in these papers. The positive phase mismatch due to the free electrons was also analyzed in the cases where HHG was effected with infrared and ultraviolet radiation. The significant difference between the phase mismatches in these two cases gave grounds to expect an improvement in the output harmonic characteristics generated with the help of short-wavelength lasers. Similar conclusions were also reached early in the investigation of HHG in gases [94]. In this connection, a comparative analysis is in order involving the use of radiation with the wavelength two times shorter than the wavelength of the traditional source (a titanium–sapphire laser, $\lambda \approx 800$ nm).

Recently, to improve the frequency conversion efficiency for laser pulses, a two-color HHG scheme in gases was proposed [95], with both fundamental radiation and its second harmonic used as a pump. The subsequent investigations into the use of the second harmonic to improve the phase matching and optimize electron trajectories revealed several new features of this process [96, 98]. Similar studies could also be undertaken in plasma HHG experiments, which would determine the feasibility of generating attosecond pulses in this experimental setup. In this connection, there is good reason to study in-plasma HHG under short-wavelength irradiation in greater detail.

In this section, we analyze the results of HHG research involving the second harmonic of titanium–sapphire laser radiation ($\lambda \approx 400$ nm). The experimental setup for HHG was described in Section 2. In this case, the main difference consists in the use of driver radiation pulses with the following parameters: $E = 5$ mJ, $t = 35$ fs, $\lambda_{fp} = 400$ nm, and the spectral width 9 nm.

A characteristic feature of the harmonic distribution in the case of 400 nm pulses was the absence of a plateau-like pattern typical for 800 nm radiation, which was observed only from beryllium plasmas in this case ($H_c = 31$, $\lambda = 12.9$ nm) [98]. The harmonics emanating from a silver plasma were much lower in intensity (in comparison with those for 800 nm radiation converted in Ag plasma) and the highest harmonic order was low (17). A comparison with the harmonics in the plateau region generated by 800 nm radiation in silver plasmas showed an approximately tenfold decrease in conversion efficiency for the doubled-frequency radiation [73].

In silver plasmas, the measurements of harmonic parameters revealed a fourfold decrease in the highest harmonic order for 400 nm radiation in comparison with 800 nm radiation. In the latter case, the highest generated harmonic order was 60 [39, 42, 90]. In this case (a two-fold shortening of the laser wavelength), the three-stage HHG model implies an eightfold lowering of the highest harmonic order (because $H_c \propto \lambda^3$). Similar departures from this dependence were observed for an aluminum target (the 15th and 43rd harmonics in the conversion of 400 nm and 800 nm wavelength pulses).

Several mechanisms may underlie this discordance. One of them may be related to the participation of different plasma components (atoms, singly and doubly charged ions)

in HHG with 400 and 800 nm pulses. Because the highest attainable harmonic order depends linearly on the intensity of the radiation being converted, this parameter should be compared for equal intensities of the 400 and 800 nm pulses. In the experiments under discussion, the intensity of the second harmonic of titanium–sapphire laser radiation was significantly lower than the fundamental radiation intensity owing to the low efficiency of conversion to the second harmonic (the corresponding pulse energies were 5 and 50 mJ). Another reason may lie with the fact that the cubic wavelength dependence holds only for very high harmonic orders. Furthermore, a role of its own may be played by a difference in defocusing caused by ionized plasmas at these two wavelengths. The departure from the cubic dependence may also be attributed to the weaker free-electron effect on the phase matching between the harmonics and the fundamental wave in the case of shorter-wavelength radiation.

The generation of enhanced individual harmonics was observed in some of the specimens, as with 800 nm radiation (see Section 3). The enhanced harmonics were generated near ion resonances with high oscillator strengths. Figure 8a depicts such a profile, which clearly shows the enhancement of the 8th harmonic ($\lambda = 44.4$ nm) in tin plasma, exceeding the intensities of the neighboring harmonics by a factor of eight. Similar enhancement in tin plasma for 800 nm pulses was discussed in Section 3. In the case of 400 nm radiation, a significant role in the enhancement of the 9th harmonic ($E_{ph} = 27.92$ eV) might also be played, along with the above transitions, by the $4d^{10}5s5p \rightarrow 4d^{9}5s5p^{2}$ (28.33–28.71 eV) transitions of Sn III ions due to large gf parameter values [87].

Observed in chromium plasmas was the enhancement of the 15th harmonic (Fig. 8b), which was due to the effect of the short-wavelength wing of a group of $3p \rightarrow 3d$ transitions of singly charged chromium ions, as with the enhancement of the 29th harmonic of 800 nm radiation [34, 73, 83].

The highest harmonic order generated in Mn plasmas turned out to be substantially lower than that for the 800 nm pulse conversion (respectively the 21st and 101st harmonics). In the harmonic spectrum of 400 nm pump radiation, the 17th harmonic stood out, exceeding the neighboring-order harmonics by a factor of six (Fig. 8c). The enhancement of a single harmonic in this case was in sharp contrast to the enhancement of a group of harmonics when 800 nm pulses were used (see the inset in Fig. 8c). The generation of harmonics of 800 nm radiation in manganese plasmas is discussed at length in Section 5.4. Here, we emphasize that the intensities of the 33rd- to 41st-order harmonics were three times higher than the neighboring harmonic intensities. To date, the 17th harmonic of 400 nm radiation ($\lambda = 23.5$ nm, $E_{ph} = 52.7$ eV) corresponds to the highest photon energy among the enhanced harmonics.

Variations in the 800 nm radiation chirp in these experiments involving 400 nm radiation did not lead to a harmonic wavelength shift, which underlies variations in the quasi-resonance conditions for the enhancement of individual harmonics. This was due to the narrow spectral width (9 nm) of the 400 nm pulses, which did not permit substantial shifts of the harmonic spectrum.

The use of shorter-wavelength sources offers several advantages in the frequency conversion of laser radiation by way of HHG. As noted above, an important feature of HHG by shorter-wavelength radiation is a smaller phase mismatch between the harmonic and pump radiation waves owing to a weaker free-electron effect on the phase

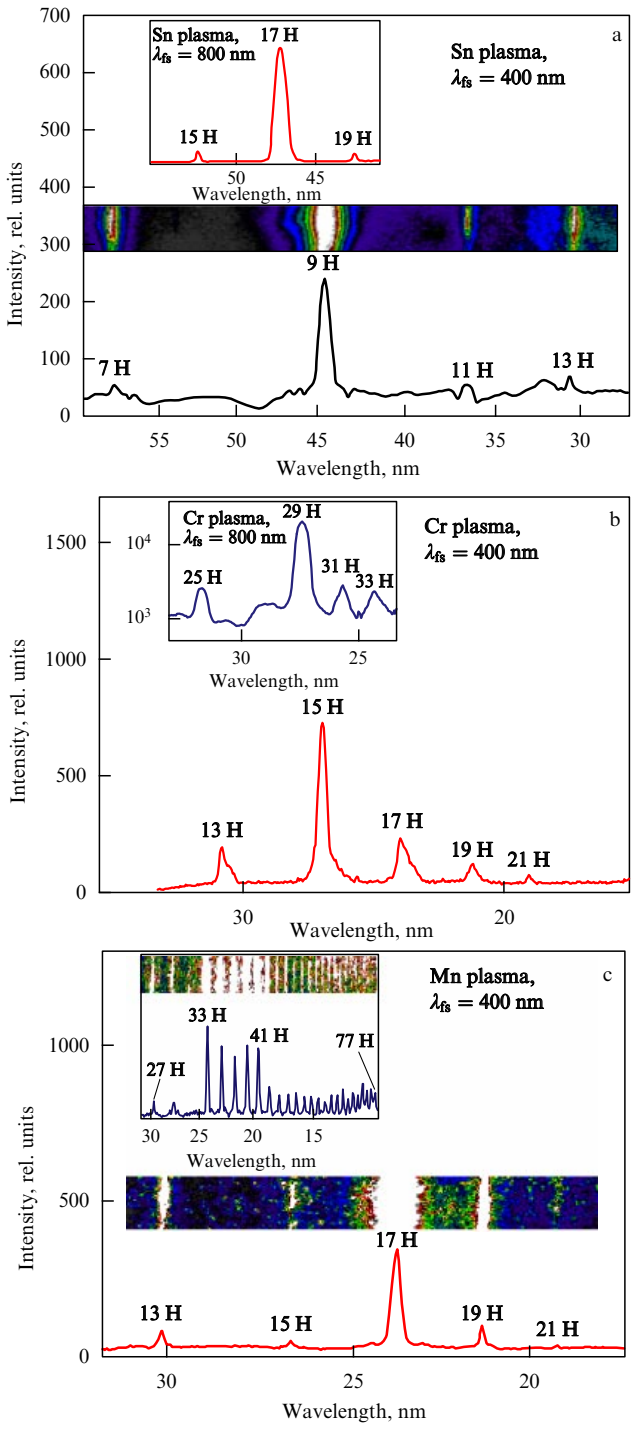

Figure 8. Enhancement of the individual harmonics of 400 nm radiation propagating through Sn (a), Cr (b), and Mn (c) plasmas. For comparison, the insets show the enhancement of the corresponding harmonics or groups of harmonics with the use of 800 nm radiation.

matching conditions. For high-order harmonics, the phase mismatch is determined primarily by the free-electron effect ($\Delta k = (n^2 - 1)(\omega_p)^2/2nc\omega$, where ω_p is the plasma frequency, n is the harmonic order, c is the speed of light, and ω is the frequency of laser radiation). For the average density of the laser flame $N = 2 \times 10^{17}$ cm^{-3} most frequently used in plasma HHG experiments and a unit degree of ionization (which corresponds to the optimal plume density in the region of interaction with the femtosecond pulse), the phase

mismatch amounts to about 90 cm^{-1} (for 400 nm pulses). The corresponding coherence length for harmonics up to the order 21 (i.e., up to $\lambda \sim 19$ nm) is equal to 0.7 nm, which is comparable to the dimensions of the plasma used (0.6 mm). At the same time, for 800 nm pulses, the corresponding phase mismatch caused by free electrons permits attaining phase matching only for harmonics with wavelengths no shorter than 38 nm. These estimates show that shorter-wavelength sources are advantageous from the standpoint of forming favorable conditions for phase-matched energy conversion to shorter-wavelength harmonics (the free-electron density being the same).

Experiments with 400 nm pulses revealed both the advantages and disadvantages of using short-wavelength radiation for HHG in laser-produced plasmas. The harmonic orders attained in these experiments did not exceed the orders of harmonics generated with 800 nm radiation. Meanwhile, among the potential advantages of using short-wavelength radiation are high conversion efficiencies in some spectral regions. In particular, the low-order harmonics of 400 nm radiation correspond to the medium-order harmonics of the 800 nm pump, and the generation of harmonics in the 100–200 nm wavelength range would be expected to exhibit higher efficiency under short-wavelength pumping. A higher coherence and shorter duration in the case of the second harmonic of titanium–sapphire laser radiation may also be rated among the virtues in this spectral range, because they afford a better phase matching between the harmonics and the fundamental wave.

The above property of short-wavelength radiation, which diminishes the adverse effect of free electrons, may be validly used if a high energy efficiency of conversion to the second harmonic is attained with nonlinear crystals. Meanwhile, the efficiency of conversion to the second harmonic in the case of femtosecond pulses and thin nonlinear crystals (required to prevent pulse lengthening due to group velocity dispersion of the waves under conversion) is still insufficiently high (~ 20–25%), which is a limiting factor in using this radiation for XUV harmonic generation.

5. Features of high-order harmonic generation in B, Ag, Au, Mn, and V plasmas

As noted in the Introduction, one of the principal goals of HHG studies is the search for plasma media that allow maximizing the generated harmonic orders and increasing the energy of the short-wavelength converted radiation pulses. In this section, we analyze the frequency conversion of laser radiation in the plasmas of different materials for the purpose of reaching this goal.

5.1 Boron

Two HHG schemes were used in studies of laser radiation frequency conversion in boron plasmas. In the first (orthogonal) scheme, which was used in the majority of HHG investigations, a part of the uncompressed titanium–sapphire laser radiation generated the plasma, following which femtosecond radiation was focused into the plasma from an orthogonal direction with a certain delay. In the second (longitudinal) scheme, a subnanosecond pulse was focused onto a surface region adjacent to a bore drilled in the target and produced the plasma, following which a second (femtosecond) pulse was directed parallel to the first one and passed through the plasma and the bore. The harmonics

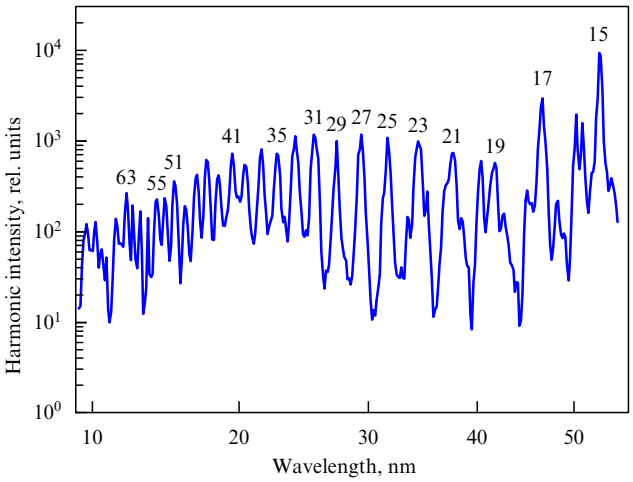

Figure 9. Spectrum of harmonics generated in boron plasma when using the orthogonal scheme.

generated in this case were recorded in the manner described in Section 2.

High-order harmonics up to the order 63 ($\lambda = 12.6$ nm [30]) were observed in experiments with boron plasmas conducted following the orthogonal scheme. A plateau-like pattern showed up in the distribution of harmonics of the orders 21 (Fig. 9) and was similar to the distribution of harmonics in numerous experiments with 'gas' harmonics. The efficiency of conversion to harmonics varied from 10^{-4} (for the third order) to 10^{-7} for harmonics located in the plateau region. The plateau-like pattern vanished when the prepulse intensity at the target exceeded some limit at which a large number of free electrons were generated and a continuum was observed in the plasma glow. The highest harmonic order did not then exceed 19. With a further increase in the prepulse intensity at the target, intense lines of doubly charged ions along with strong continuum radiation appeared in the boron plasma spectrum, which did not permit observing harmonics with wavelengths shorter than 65 nm.

HHG was optimized by varying the experiment geometry, with the femtosecond pulse focusing varied from 'weak' ($b = 4.8$ mm, $L_p \approx 0.6$ mm, $b \gg L_p$, where b and L_p are respectively the confocal parameter of the focused radiation and the plasma length) to 'strong' ($b = 1.2$ mm, $L_p \approx 0.6$ mm, $b \propto L_p$). In this case, the order of generated harmonics somewhat increased (the 65th harmonic, $\lambda = 12.24$ nm), as did the conversion efficiency in the plateau region (5×10^{-7}).

An analysis of the harmonic radiation generated using the second (longitudinal) HHG scheme demonstrated the crucial role of the characteristics of heating prepulse radiation in the formation of optimal conditions for the frequency conversion of laser radiation. For a low prepulse energy, a power-law dependence with the exponent equal to 3.5 was observed for the dependence of harmonic intensities on the prepulse intensity near the target. Up to 57th-order harmonics were generated in this investigation. However, the conversion efficiency remained low (10^{-7} [100]).

5.2 Silver

In the case of silver plasma, the plateau-like pattern was observed for harmonics of the orders higher than 9 (see Fig. 3). The conversion efficiency (1×10^{-6}) was much higher than

the conversion efficiency in the boron plasma under similar experimental conditions. The calibration of the recording instruments in the high- and low-order harmonic regions enabled performing absolute measurements of the conversion efficiency [42]. The subsequent optimization of this experiment led to an appreciable increase in the HHG efficiency in the plateau region (8×10^{-6}), which turned out to be comparable to the conversion efficiency in gas-jet sources.

An important characteristic of this process is the dependence of the highest generated harmonic order on the intensity of the femtosecond pulse. For Ag plasma, this dependence $H_c(I_{fp})$ was linear and reached saturation for $I_{fp} = 3.5 \times 10^{14}$ W cm^{-2}. This intensity of the 150 fs pulses is much higher than the tunnel ionization intensity for neutral silver atoms. The results of investigations show that the role of free electrons generated in the ionization of neutral atoms is insignificant, owing to their low density. Because the ionization of neutral atoms does not lead to a saturation of the above dependence and does not entail a substantial phase mismatch, self-defocusing, or suppression of the peak intensity in the plasma region, this saturation (the 57th harmonic) may be caused by the further ionization of singly charged ions and an increase in the free-electron density. Calculations of the tunnel ionization threshold for singly charged silver ions (2.1×10^{14} W cm^{-2}, $I_{2i} = 21.48$ eV) show that it is nearly the same as the intensity at which the dependence $H_c(I_{fp})$ is saturated.

Subsequent experiments with silver plasmas carried out using 48 fs 795 nm pulses showed an increase in H_c (the 61st harmonic, $\lambda = 13$ nm (Fig. 10)). The conditions for harmonic generation were optimal when the distance between the radiation–plasma interaction region and the target surface was equal to 100 – 200 μm, depending on the order of the harmonic generated. The optimal distance was dependent on the temporal delay between the pulses. These experiments, like the previous ones, exposed the adverse effect of excessive prepulse intensity near the target, resulting in a lowering of the conversion efficiency (for $I_{pp} > 3 \times 10^{10}$ W cm^{-2}) or a total loss of the HHG conditions (for $I_{pp} > 8 \times 10^{10}$ W cm^{-2}) [39].

An important point in these investigations was to determine the optimal HHG conditions for different positions of the focal plane of the lens that focused the fundamental femtosecond beam into the Ag plasma. The dependence of harmonic intensities on the location of the focus relative to the plasma plume was largely determined by the pulse energy and by the intensity at the focus of the lens in use. For a low intensity, a single maximum was observed in the dependence $I_h(z)$ (where I_h is the harmonic intensity and z is the longitudinal coordinate), occurring when the focal region coincided with the plasma plume. But for a high femtosecond radiation intensity, this dependence had two peaks: the first, the smaller one, when the focal plane was located in front of the plasma plume, and the greater one, when the focal plane was located behind the plume. Under this irradiation intensity, focusing into the plasma region gave rise to a substantial additional ionization of the plasma plume and a subsequent intense glow in the XUV range. In this case, the emergence of excess free electrons and phase self-modulation were responsible for the loss of the phase matching between the fundamental radiation and harmonic waves and for a consequential sharp decrease in the HHG efficiency.

When the focal point is behind the nonlinear medium, one would expect a change in the spatial form of laser radiation (from a Gaussian distribution to a more flat distribution in the central region of the beam) due to a higher free-electron density in the paraxial region, which leads to defocusing of this part of the beam. These conditions are analyzed at length in Ref. [101]. When the nonlinear medium is located in front of the focal plane of the femtosecond pulse, the central part of the laser beam experiences nonlinear negative refraction caused by free electrons, which increases the divergence of this beam region. At the same time, the 'wings' of the spatial distribution of this beam are still focused into the plasma. In this case, it is possible to attain a phase-matched energy transfer from the pump wave to harmonic waves over a longer path in the plasma, which is attended with an increase in harmonic intensities. This was earlier observed in gas media [102, 103].

The importance of careful control over the prepulse and main pulse energies for efficient HHG was demonstrated in subsequent experiments with shorter (35 fs) pulses. Variations in spectral harmonic widths with increasing the prepulse intensity were observed in experiments with Ag plasmas [99]. Figure 11 shows the spectral widths of the 17th, 25th, and 43rd harmonics as functions of the prepulse intensity. The form of these dependences clearly shows that while the spectral width of the lower-order harmonics increases with I_{pp}, this parameter remains invariable for higher-order harmonics.

Plasma plume characteristics were calculated using the HYADES code. This one-dimensional code was devised earlier for calculating laboratory plasmas produced under the action of high-power energy sources. The code was elaborated to suit the following requirements: (i) convenience in use by an experimenter; (ii) recourse to simple but reliable approximations involving different physical models; (iii) the possibility of modifying it with relative ease and

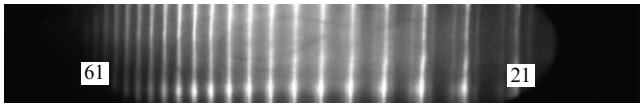

Figure 10. Distribution of harmonics generated in a silver plasma with the use of 48 fs pulses.

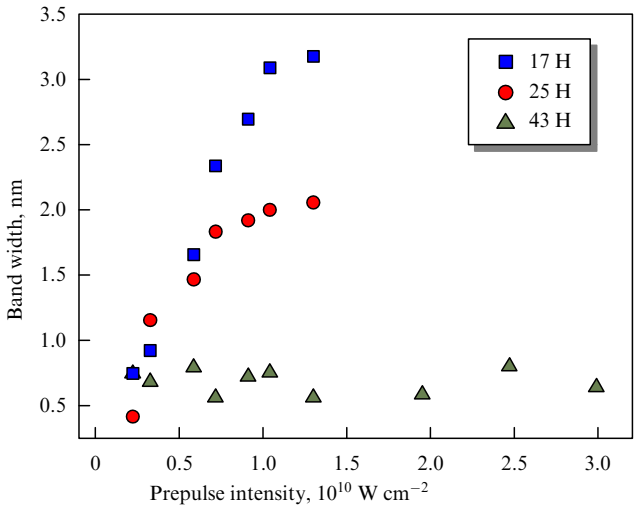

Figure 11. Dependence of the spectral widths of the 17th, 25th, and 43rd harmonics on the intensity of 35 fs pulses.

Table 1. Calculated characteristics of silver plasmas.

Prepulse intensity, 10^{10} W cm^{-2}	0.3	0.59	0.9	1.3	1.95	2.6	3.25
Electron density, 10^{17} cm^{-3}	0.89	2.56	3.2	4.0	5.79	6.33	8.0
Ion density, 10^{17} cm^{-3}	0.89	2.56	3.17	3.41	4.45	4.55	5.06
Ionization degree	0.5	0.7	1.01	1.17	1.3	1.39	1.58

including new models for consideration; and (iv) the possibility of using different computer operating systems. Recent modifications to this code have allowed obtaining more realistic values of calculated plasma parameters, in particular, of the temperatures in the range of several electronvolts. Elaborated by Larsen and Lane [104], these modifications of the HYADES code were later used to calculate the dynamics of deposition with the use of a plasma plume [105], to model different plasma instabilities [106], to optimize the characteristics of tenuous plasmas for various applications [107], etc.

Experiments in harmonic generation from silver plasmas and harmonic brightness variations (in other words, spectral width variations), as well as calculations by the HYADES code showed that initially (for a low prepulse intensity, $I_{pp} < 0.9 \times 10^{10}$ W cm^{-2}), the degree of plasma ionization lies in the range from 0.5 to 1 (Table 1). In this case, the plasma consists of neutral atoms and singly charged ions responsible for HHG. For prepulse intensities in the range $(0.9-3) \times 10^{10}$ W cm^{-2}, the ionization level becomes higher than unity. Under these conditions, the plasma consists primarily of singly charged silver ions and of a small fraction of doubly charged ions. In this case, spectral broadening of lower-order harmonics is observed, while the spectrum of higher-order harmonics remains invariable. For intensities above 3×10^{10} W cm^{-2}, the ionization level exceeds 1.5. In this case, an increase in the free-electron density hinders subsequent HHG due to a phase mismatch of the participating waves.

5.3 Gold

Analysis of laser-produced plasma characteristics plays an important role in the optimization of frequency conversion of high-power laser radiation. One such characteristic is the spectral composition of plasma glow in the visible and UV ranges. Early in the investigation of HHG in laser-produced plasma, the spectrum was analyzed proceeding from time-integrated spectral characteristics of the plasma plume. To state it in different terms, the recorded spectrum of the plume was accumulated during the whole period of its glow [35]. However, recent investigations of HHG in the plasma produced on the surface of several targets involved a technique of analysis of the plasma plume at different stages of its development [108]. This enabled revealing several features in the dynamics of plasma overexcitation under femtosecond irradiation for different targets and intensities of the heating pulse. In what follows, we give the results of an analysis of the plasma produced on the surface of gold, which was performed for the purpose of optimizing its characteristics for HHG.

The interval between each spectrum measurement was 20 ns, beginning from the onset of Au plasma excitation to the moment at which the plasma appreciably recombined under the conditions optimal for HHG (150 ns). These investigations were carried out for both 'optimal' and 'nonoptimal' plasmas. The term 'optimal' characterizes the plasma plume state that corresponds to the maximum HHG efficiency. In a nonoptimal plasma, the efficiency is significantly lower due to the effect of several limiting factors. The plasma spectrum was measured in a narrow UV range (266–295 nm), in which it was possible to trace the excitation of singly charged ions. The optimal plasma afforded the generation of a plateau-like harmonic distribution, the generation of highest-order harmonics being observed in this case.

Figure 12 shows the dynamics of the UV spectrum of gold plasma irradiated by femtosecond radiation 100 ns after the onset of plasma development. The decay times for the lines of excited neutral atoms were appreciably different from the decay times of ionic lines. It can be seen from Fig. 12 that the intensities of Au II lines (280.20 nm, 282.25 nm, and 291.18 nm), which are excited under these conditions, decrease rapidly, while the emission in the lines arising from neutral gold atoms (267.59 nm and 274.82 nm) is sufficiently longer than the emission of ionic lines. It can also be seen from these spectra that the main pulse, which arrives 100 ns after the onset of plasma formation, primarily excites the ionic lines, while the lines of neutral atoms do not undergo significant changes [74].

A different picture was observed in UV-spectrum dynamics with an increase in the prepulse intensity at the target surface. Increasing this parameter from $1\times$ $\times 10^{10}$ W cm^{-2} to $(2-3) \times 10^{10}$ W cm^{-2} resulted in a substantial strengthening of the plasma emission. Along with an approximately four-fold increase in ionic line intensities, there emerged other spectral features arising from additional ion transitions in the spectrum of gold. The UV plasma spectra for optimal and nonoptimal harmonic generation conditions 90 and 100 ns after the onset of plasma formation were significantly different. A similar picture had also to be expected for the spectral distribution in the EUV spectral range ($\lambda < 30$ nm). The experimental conditions did not permit analyzing the dynamics of the plasma spectrum with a temporal resolution in this range, but the emergence of intense ionic lines in the domain of plateau-like harmonic distribution, which was seen from the integral spectra of harmonics and plasma, led to a substantial decrease in the intensity of the harmonics and sometimes to their complete disappearance. In particular, a relatively small increase in the prepulse intensity at the target surface (for 1×10^{10} to 2.5×10^{10} W cm^{-2}) entailed a 2.5-fold decrease in the intensity of the 13th harmonic.

The analysis conducted allowed optimizing the HHG by selecting the most appropriate intensities for the prepulse and the main pulse, as well as the time delay between them. This optimization enabled reducing the effect of the main HHG limiting factor in radiation conversion in plasmas—the excess free-electron density, which is responsible for a phase mismatch and self-defocusing. Optimization of this kind permitted advancing the harmonics generated in the Au plasma towards shorter wavelengths. Under these conditions, the generated harmonic order was as high as 53 ($\lambda = 15.09$ nm). A comparison of the conversion efficiencies for Ag and Au plasmas showed that in the latter case, the intensities of the 25th to 49th harmonics were several times lower. The conversion efficiency in the plateau region in gold plasma was equal to 2×10^{-6}.

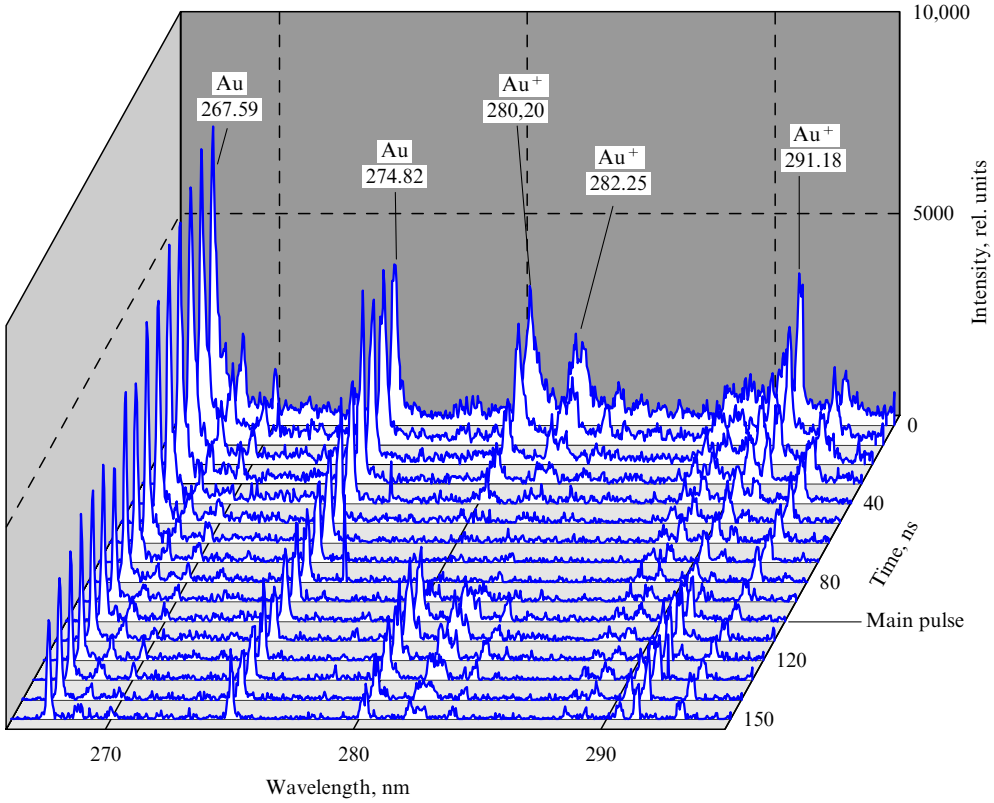

Figure 12. Dynamics of the UV emission spectra of gold plasma, $I_{pp} = 1 \times 10^{10}$ W cm^{-2}.

These investigations demonstrated the advantages of analyzing plasma at different stages of its development with a high temporal resolution. The technique outlined above is the first attempt to optimize the characteristics of a plasma used as a nonlinear medium in HHG, proceeding from the analysis of laser-produced plasma dynamics in the course of its development.

5.4 Manganese and vanadium

The relation between the highest generated harmonic order and the ionization potential I_i of the particles participating in HHG was analyzed in Refs [35, 39, 41]. In the majority of cases, the harmonic generation in the plasma was effected in the interaction of ultrashort pulses with singly charged ions. In this case, the second ionization potential of target atoms should be regarded as a parameter that controls H_c. The empirical relation $H_c \approx 4I_i - 32.1$ was confirmed by different groups [35, 39, 41] in the numerous H_c parameter measurements using titanium–sapphire lasers that generated pulses of different durations (35, 48, and 130 fs) (Fig. 13). When singly charged ions play a decisive role in HHG, this relation implies that the shortest-wavelength harmonics is generated in plasma plumes produced on the surfaces of targets that have the highest second ionization potentials. The emergence of an excess electron density due to the subsequent ionization of singly charged ions with an increase in the laser radiation intensity causes the dependence $H_c(I_{fp})$. However, recent investigations of HHG in manganese plasma revealed new interesting features of this process. As in earlier investigations, harmonics up to $H_c = 29$ were generated in this medium, which corresponded to the empirical relation $I_{2i} = 15.64$ eV for the second Mn ionization potential (Fig. 13). But under subsequent changes of plasma characteristics (when the manganese target surface was irradiated by subnanosecond pulses of a higher intensity than that corresponding to the optimal plasma for the majority of targets ($I_{pp} \approx 1 \times 10^{10}$ W cm^{-2}), the number of generated harmonics increased significantly. Harmonics up to the order 101 were experimentally observed (Fig. 14). In this case, instead of the plateau-like distribution of harmonics of the

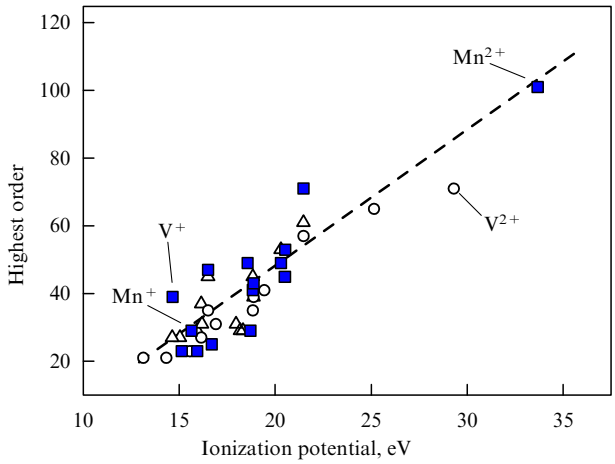

Figure 13. Dependence of the highest generated harmonic order H_C on the ionization potential of singly and doubly charged ions participating in HHG. The dashed line corresponds to the relation $H_c \approx 4I_i$ [eV]-32.1 for the highest harmonic order. The squares represent the data obtained at the Institut National de la Recherche Scientifique (Canada) [41], the circles stand for the data obtained in the Institute for Solid State Physics (Japan) [35], and the triangles are the data obtained at the Centre for Advanced Technology (India) [39].

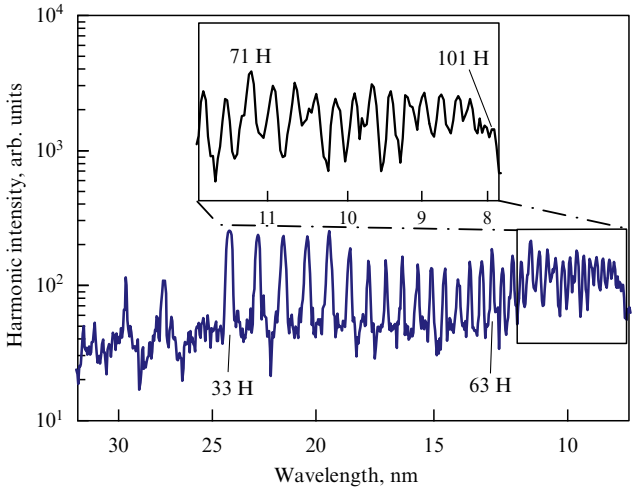

Figure 14. Harmonic spectrum obtained from manganese plasma ($I_{pp} = 3 \times 10^{10}$ W cm^{-2}, $I_{fp} = 2 \times 10^{15}$ W cm^{-2}). The inset shows the spectral region between the 67th and the 101st harmonics.

orders from 15 to 29 (observed at moderate target irradiation intensities), there emerged another plateau (for harmonics of the orders from 33 to 93) followed by a sharp decrease in the intensities of higher-order harmonics up to the order 101 ($\lambda = 7.9$ nm) [41]. The new value of H_c was in satisfactory agreement with estimates following from the empirical relation $H_c(I_i)$ with the inclusion of doubly charged ions and the third ionization potential of manganese $I_{3i} = 33.67$ eV (see Fig. 13). We note that increasing the prepulse intensity ($I_{pp} > 3 \times 10^{10}$ W cm^{-2}) when investigating plasmas produced at the surface of other targets entailed a substantial impairment of the generated harmonic pattern, such that high-intensity XUV spectral lines of the plasma emission did not permit recording harmonics with wavelengths shorter than a certain value.

As in the case of silver plasma, calculations were performed with the aid of the HYADES code for two targets (Mn and Au) to analyze the reasons why the HHG picture was different for different targets. The development of plasma on the surface of these targets was analyzed, which enabled estimating the electron and ion densities as well as the ionization plasma state at the distance 300 μm from the target surfaces 100 ns after excitation by a subnanosecond pulse (Table 2). As may be inferred from these data, even for $I_{pp} = 1 \times 10^{10}$ W cm^{-2}, there occurred a substantial difference in the ionization state of the plasmas of these two targets, which resulted in different nonlinear optical responses of the Mn and Au plasma plumes. Under this irradiation intensity, the ionization state of the gold plasma exceeded unity, which led to the emergence of additional free electrons due to ionization of singly charged ions. The electron–ion density ratio in the Au plasma continued to increase with the prepulse intensity at the target surface to become greater than 3 for $I_{pp} = 5 \times 10^{10}$ W cm^{-2}. The increase in the free-electron density in this case hampered the generation of harmonics and an increase in H_c.

A qualitatively different picture emerged in the calculation of manganese plasmas. According to the calculated data, doubly charged ions should occur only when $I_{pp} > 3 \times 10^{10}$ W cm^{-2}, limiting an increase in the free-electron density at lower intensities. This circumstance led to a weaker manifestation of femtosecond-pulse self-defocusing and

Table 2. Calculated characteristics of manganese and gold plasmas.

Prepulse intensity, 10^{10} W cm^{-2}	Target	1.04	2	3	5
Electron density, 10^{17} cm^{-3}	Mn	1.3	3.25	3.77	6.13
	Au	7.32	14.2	18.5	25.2
Ion density, 10^{17} cm^{-3}	Mn	1.3	3.25	3.77	4.50
	Au	4.7	6.03	6.8	7.52
Ionization degree	Mn	0.62	1.0	1.0	1.36
	Au	1.56	2.35	2.72	3.35

phase mismatch (in comparison with those for gold plasmas), which in turn led to an increase in H_c.

A conclusion following from the above analysis is that the optimal plasma HHG conditions must be determined by calculating plasma characteristics and analyzing the plasma state with recourse to the spectroscopic technique with a high temporal resolution described in Section 5.3. This approach allows finding plasmas that favor further advancement to the short-wavelength spectral domain. The validity of this approach was confirmed by the recent study of HHG in vanadium plasmas. According to estimates relying on the empirical relation (for the ionization potential $I_{2i} = 14.65$ eV), the highest value of generated harmonic order was expected to lie in the thirties, considering the participation of singly charged ions in HHG. In the experiment, which provided support for these calculated data, it was possible to observe the 39th harmonic of 800 nm radiation (see Fig. 13). Meanwhile, recent investigations of HHG in vanadium plasmas demonstrated the feasibility of substantially increasing H_c in the further optimization of the plasma plume and the intensity of the pump radiation. Up to 71st-order harmonics were obtained in this case [40]. Following the approach described in this section and considering the proximity of the plasma characteristics of V and Mn (revealed in the course of HYADES code-assisted calculations), it may be suggested that the HHG in the optimized vanadium plasma proceeded with the participation of doubly charge ions ($I_{3i} = 29.31$ eV). In view of the empirical relation, the generation of up to 79th-order harmonics can be expected in this case (see Fig. 13), which is close to the experimental value (the 71st harmonic). A similar approach to the quest for media wherein harmonics are generated with the participation of doubly charged ions afforded a substantial increase in the harmonic order for HHG in titanium plasmas [109].

6. High-order harmonic generation in plasmas produced by laser pulses of various durations

The results of the investigations outlined in Sections 2–5 exposed the decisive role of plasma characteristics in attaining the highest efficiency of coherent radiation conversion to the XUV band as well as in generating the highest-order harmonics. For this, different techniques have been used, such as (i) an analysis of the ionization state and of electron and ion densities reliant on HYADES code-assisted calculations [99]; (ii) investigations of integral laser-produced plasma spectra [35, 39] and of the time-resolved plasma spectra with the use of a high-speed technique allowing the laser flame to be analyzed with a high temporal resolution [67, 74]; (iii) measurements of the divergence of a femtosecond beam

transmitted through laser-produced plasma [110], and (iv) an analysis of nonlinear optical plasma parameters with the use of the Z-scanning technique [110].

Meanwhile, several important characteristics such as the duration of the heating prepulse were not varied in the plasma production. The overwhelming majority of investigations of plasma HHG were carried out using pulses several hundred picoseconds long. The conclusion drawn in that case involved determination of the 'optimal' prepulse intensity at the target surface ($\sim (1-4) \times 10^{10}$ W cm^{-2}, depending on the physical material properties [32, 35, 99]), which afforded the highest value of H_c as well as the highest attainable HHG efficiency in the plateau domain. In this connection, it seemed expedient to undertake a comparative analysis of HHG in plasmas produced by pulses of various durations: these investigations could allow determining which parameter of the heating radiation (the pulse energy or the radiation intensity at the target surface) played the crucial role in optimal plasma formation.

Another interesting point is the effect of the target material atomic number Z on the HHG efficiency for different delays between the participating pulses. It is important to determine whether the target characteristics affect the optimal delay between the prepulse and the femtosecond pulse. It may be expected from general considerations that the HHG dynamics would be different for 'light' and 'heavy' target atoms (i.e., for low- and high-Z materials), because the heating, melting, evaporation, and escape from the target surface, as well as the subsequent cooling and recombination of target particles depend on the atomic weight and the target density. The difference in the escape velocity and recombination between light and heavy atoms and ions of laser-produced plasmas may have a pronounced effect on the plasma density characteristics at different distances from the target and under delay variations. In this case, optimizing the delay between the prepulse and the pump pulse would favor the attainment of better characteristics of radiation conversion for light or heavy targets.

In this section, we analyze the results of investigations of HHG in plasmas produced on the surface of low-, medium-, and high-Z targets irradiated by radiation pulses varied over five orders of magnitude in duration (from 160 fs to 20 ns). These investigations showed that plasma formation is crucial in the optimization of HHG and the optimal plasma characteristics are largely determined by the pulse energy, while the radiation intensity at the target surface affects the dynamics of harmonic generation to a much smaller degree. In the course of these experiments, it was possible to reveal the difference in HHG in plasmas produced at the surfaces of targets consisting of light or heavy elements, when the delay between the pulses becomes the controlling factor for the attainment of efficient harmonic generation [111].

The setup of the experiments described below was similar to the previous ones. Initially, a 210 ps prepulse was used. The duration of this prepulse was varied by way of its compression in an additional compressor. In particular, in the HHG research in this case, 160 fs and 1.5 ps pulses were used. The energy of these pulses was maintained at about the same level (10 mJ). The pulse was focused onto the target using a spherical (or cylindrical) lens. Materials with a high (silver, barium), medium (zinc, nickel, manganese), and low (graphite, boron, lithium) atomic number were used as targets. The intensity of 210 ps pulses at the target surface was kept in the interval $I_{pp} = (1-5) \times 10^{10}$ W cm^{-2}. In the cases of 160 fs and 1.5 ps pulses, the radiation intensity at the target surface was much higher, because these investigations were carried out under the same experiment geometry and the energies of the prepulses of different durations were about the same.

After a corresponding delay, the focused radiation of the main pulse (115 fs, 20 mJ, 795 nm) passed through the plasma produced. Because the highest attainable intensity (6×10^{16} W cm^{-2}) of this pulse in the focal plane was much higher than the tunnel ionization thresholds for singly and doubly charged plasma ions, the position of the focal region (behind or in front of the target) was chosen in such a way as to maximize the harmonic intensities. For this position, the intensity of the main pulse in the plasma plume was in the range $7 \times 10^{14} - 3 \times 10^{15}$ W cm^{-2}. These experiments were performed under 'weak' focusing ($b > L_p$).

Figure 15 shows the results of investigation of H_c as a function of the pulse duration for heavy (Ag ($Z = 47$)), intermediate (Zn ($Z = 30$)), and light (B ($Z = 5$) and Li ($Z = 3$)) targets. These experiments suggest that there is a substantial difference in harmonic characteristics among these three groups of targets. For heavy targets (and for the majority of medium-Z targets), no variation in the highest generated harmonic order was observed when 160 fs, 1.5 ps, and 210 ps prepulses were used. In several instances, 20 ns pulses of the second harmonic of an yttrium–aluminum garnet laser were used as a heating prepulse. The use of these pulses did not entail substantial changes (in the case of heavy targets) in H_c.

However, an essential dependence of H_c on the duration of the heating pulse was observed in the case of light targets. But even in these circumstances, no fundamental limiting factors were revealed that led to a strong violation of HHG conditions for a substantial variation of the heating radiation intensity, which amounted to five orders of magnitude. The only exception was the lithium plasma, in which high-order harmonics were generated only with the use of long (210 ps) prepulses and short delays. In this case, the main distinction in HHG characteristics consisted in the length of delay between the heating and main pulses. These investigations demonstrated that the prepulse energy plays the decisive role in the formation of optimal conditions for plasma HHG.

The integral spectra of laser-produced plasma in the visible and ultraviolet spectral domains showed that the general spectral line distribution pattern was about the same despite the difference in duration of the prepulses that generate the plasma on the target surfaces. The Mn- and Ag-plasma emission spectra in the visible and near-ultraviolet spectral ranges excited by 160 fs, 1.5 ps, and 210 ps pulses showed that the length of the heating radiation pulse had no appreciable effect on the dynamics of laser plume emission and that the leading role in plasma excitation was played by the pulse energy under the conditions of a nonlinear medium close to the optimal one for HHG. The same is true of plasma emission in the XUV range, which is an indication that the laser plume characteristics are about the same for substantially different prepulse intensities at the target surface excited by radiation with different pulse lengths.

The HHG efficiency depended to a large measure on the time delay between the prepulse and the main pulse. For very short delays (5 ns and less), harmonic generation was not observed due to the insufficient density of the nonlinear medium in the region of interaction with the femtosecond pulse. Under a further increase in the time delay, a substantial difference between the generation properties of light and

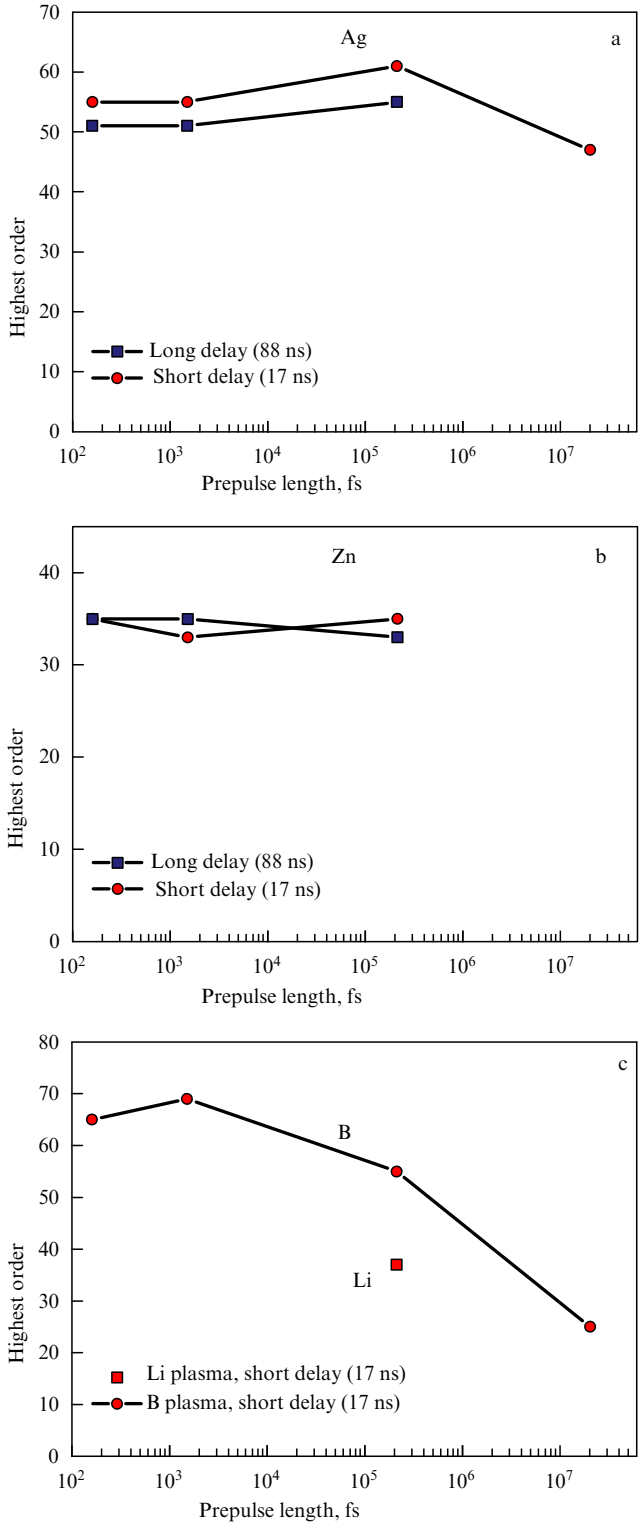

Figure 15. Highest harmonic orders generated in (a) heavy (Ag), (b) intermediate (Zn), and (c) light (Li and B) target plasmas for different delays and prepulse lengths.

heavy targets manifested itself. For a 17 ns delay, HHG was observed with the use of all the targets under investigation, while for an 88 ns delay, the harmonics were generated only in plasmas of high- and medium-Z targets (see Fig. 15). For this long delay, the harmonics were not generated in the plasmas of light targets (with the exception of graphite). We note that the values of H_c for high- and low-Z targets were about the same for short and long delays between the pulses.

This difference in generation properties may be related to the dynamic plasma characteristics for light and heavy targets. Light particles fly away from the target at a higher velocity, which may entail a lower laser-produced plasma density in the region of interaction with the main pulse several tens of nanoseconds after the onset of plasma formation. But heavier particles stay near the target (where the laser radiation frequency is converted) for a longer time. For heavy targets, the delay between the prepulse and the main pulse turned out to have a weaker effect on the generated harmonic intensities than for light targets. Therefore, in the search for possible targets, their physical parameters should be taken into account along with their spectral characteristics.

It was noted in Section 5 that the second ionization potential of targets plays an important role in determining the highest generated harmonic order. The results of investigations described in this section revealed additional target and prepulse parameters, as well as the delays between the pulses, which should be taken into account in the subsequent identification of materials whose plasmas favor the generation of highest-order harmonics with the highest conversion efficiency.

From the empirical formula that relates the highest generated harmonic order to the ionization potential of the particles participating in the conversion of laser radiation frequency ($H_c \approx 4I_i - 32.1$ [41]), it follows that the highest H_c is to be observed in a medium having the highest ionization potential of these particles. In the majority of cases, when singly charged ions played the role of the main component participating in HHG, the highest H_c values were observed in the plasma plumes of materials with the largest value of the second ionization potential (in particular, in silver and boron plasmas). At the same time, as noted in Section 5.4, the H_c parameter was seen to exceed the expected value following from the above relation, which may be attributed to the participation of doubly charged ions in the frequency conversion. The highest harmonic orders observed in this case and the third ionization potentials of these materials (vanadium and manganese) fit the above relation satisfactorily. Hence, it follows that the plasma media that favor the realization of conditions for the generation of ultimately high-order harmonics should be sought among materials with the highest third ionization potential.

The targets used in the investigations described in this section were chosen based on precisely these considerations. But the attempts to attain H_c values exceeding the highest harmonic orders (the 71st for vanadium and the 101st for manganese plasmas) reported previously were not successful in these experiments. The reason may lie with specific phase matching relations in different plasma media, which may lead to efficient HHG with the participation of doubly charged ions only in a limited number of materials, while in other plasma plumes with a high value of the third ionization potential, the effect of an excess free-electron density may largely impair the phase matching in the laser radiation frequency conversion. Laser-produced plasma is a highly complicated medium as regards its nonlinear optical properties. The behavior of this plasma system is appreciably subject to changes involving variations in the ionization state, ion and electron densities, ionization potentials, and a number of thermodynamic parameters. The processes defining the HHG efficiency in this medium are rather complex and involve

several additional factors that are nonexistent for HHG in gases. In particular, the plasma medium initially consists of neutral particles, ions, and free electrons, and the densities of these plasma constituents depend to a great extent on the prepulse and target characteristics. As noted above, an excess free-electron density (generated, in particular, in the subsequent ionization of singly charged ions) appreciably impairs the phase matching between the harmonics and the radiation under conversion.

7. Analysis of laser-produced plasma characteristics for the optimization of high-order harmonic generation

An ion medium modifies the temporal characteristics of femtosecond laser pulses owing to phase self-modulation. Furthermore, the spectral structure of high-order harmonics depends critically on the frequency modulation (chirp) of the radiation under conversion. Available from the literature are reports about investigations of the dynamics of chirped pulse propagation through ionized gas-jet sources and data about the spatial, spectral, and temporal parameters of laser radiation transmitted through such a medium, as well as the parameters of harmonics (see Ref. [112] and the references therein). Among the processes that affect the parameters of laser radiation, a prominent role is played by self-defocusing. Because self-defocusing appears to be one of the main limiting mechanisms for HHG (both in gases and in laser-produced plasmas), it was vital to analyze this process in greater detail under conditions close to the 'optimal' plasma, in which the HHG is realized most efficiently, as well as to determine the experimental conditions under which the self-defocusing effect is less significant.

In the experiments discussed below, the spatial distribution of the pump radiation ($f = 150$ fs) transmitted through the plasma plume for different plasma densities (from 5×10^{16} cm^{-3} to 2×10^{17} cm^{-3}) and laser radiation intensities was analyzed using a CCD camera in the far-field zone. The nonlinear optical characteristics of indium and molybdenum plasmas were investigated by the Z-scanning technique.

The spatial distribution of the radiation transmitted through the plasma remained invariable for low intensities of the femtosecond pulses even when the ionization threshold of target atoms was exceeded. This observation showed that the density of free carriers generated in the course of plasma production and in the subsequent ionization of neutral plasma particles induced by a femtosecond pulse is insufficient for the self-defocusing of the laser beam. A different spatial distribution pattern of the laser radiation transmitted through the plasma was observed when the thresholds for the tunnel ionization of singly and doubly charged ions were exceeded. According to calculations, the respective tunnel ionization thresholds for Mo I, Mo II, and Mo III are equal to 1.2×10^{13}, 7×10^{13}, and 2.4×10^{14} W cm^{-2}. For $I_{\rm fp} \geqslant 3 \times 10^{14}$ W cm^{-2}, the density of free electrons that emerged in the focal region in a time much shorter than the duration of the femtosecond pulse proved to be sufficient for the occurrence of self-defocusing of the laser beam. An annular structure was observed in the profile of the transmitted beam in this case, which was indicative of variations in the refractive index of the medium along the beam propagation axis.

The Z-scanning of different plasma plumes was performed similarly (Fig. 16). For low intensities of laser pulses,

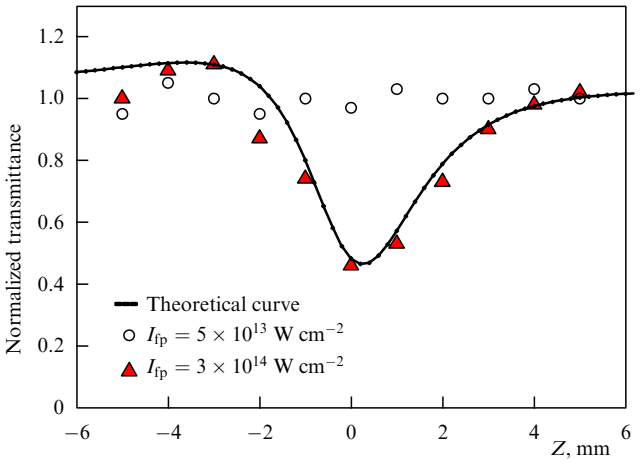

Figure 16. Z-scanning of indium plasma for low (circles) and high (triangles) intensities of femtosecond pulses. The solid curve represents the data of theoretical calculations.

the normalized transmittance of the laser radiation transmitted through the plasma and the limiting far-field aperture remained invariable. However, with an increase in the beam intensity, a specific feature showed up in the normalized transmittance, which was a small peak with the subsequent substantial lowering of transmittance through the diagram. This feature was due to the self-defocusing and nonlinear absorption effects arising from the tunnel ionization of neutral particles and ions. The setup with a limiting aperture enabled determining the magnitude and sign of the nonlinear refractive index γ as well as the magnitude of the nonlinear absorption coefficient β of the plasma plumes. For indium plasma, in particular, γ and β were respectively equal to -2×10^{-18} cm^2 W^{-1} and 5×10^{-13} cm W^{-1} [110]. The β parameter depended to a large measure on the radiation intensity in the plasma plume region, which was to be expected considering the multiphoton nature of the nonlinear absorption. In particular, four-photon absorption ($I_{\rm i} = 5.8$ eV) was the dominant process in indium plasma ($E_{\rm ph} = 1.56$ eV) and five-photon absorption in Mo plasma ($I_{\rm i} = 7.1$ eV). The four-photon absorption coefficient calculated for indium plasma was 5×10^{-42} cm^5 W^{-3}.

Investigations of the shape of the laser beam transmitted through the plasma at different radiation intensities and plasma plume densities allowed determining the role played by free electrons, which are generated during the ionization of neutral particles and ions, in changing the spatial and, accordingly, phase characteristics of the laser pulse in the focal plane. Self-defocusing and the corresponding changes of the phase characteristics of laser pulses do not permit preserving the phase matching between the harmonic and pump radiation waves throughout the path of the pulse in a nonlinear medium. The intensity of laser radiation also decreases in this case, which is caused by an increase in divergence on the beam axis in the interaction region. These effects prevent attaining favorable conditions for efficient HHG in the passage of laser radiation through the plasma, which lowers the conversion efficiency and decreases the highest generated harmonic order. Plasma investigations using the Z-scanning technique confirmed the limiting role of processes such as self-defocusing and nonlinear absorption in the conversion of the wavelength of laser pulses.

Optimizing HHG in a plasma involves fulfilling several conditions. Because the time of plasma development ranges from several nanoseconds to several hundred nanoseconds, the passage of a laser pulse should be timed to the occurrence of the 'optimally prepared' plasma. The investigations described above showed that the main parameters that must be optimized for fulfilling these conditions are the plasma density, the degree of plasma excitation and ionization, and the linear dimensions of the plasma region. The presence of excited components in the plasma may substantially strengthen the nonlinear optical response of the plasma plume. Another important parameter is the delay between the heating subnanosecond prepulse and the femtosecond pump pulse. Also noteworthy is the important role of the experiment geometry, which permits producing both a point-like plasma and a plume elongated along the axis of the pump pulse propagation. Increasing the linear dimensions of the plasma region will affect HHG due to the competition between the increase in the HHG efficiency, which is caused by the elongation of the nonlinear medium, and the reabsorption of the generated harmonics along with destructive interference, owing to the fact that the length of the medium exceeds the length of the coherent interaction of the harmonics in different spectral regions. These features were noted in the studies of HHG in indium and boron plasmas [32, 33] and in experiments involving graphite [113], magnesium [114], aluminum [115], and molybdenum [116].

8. Frequency conversion of laser radiation to far-ultraviolet radiation with the use of nanoparticle-containing plasmas

Nanoparticle research has demonstrated the feasibility of increasing the efficiency of harmonic generation with the use of cluster media. We note that the majority of previous works on HHG involving nanoparticles [63, 64, 117–129] was limited to the analysis of rather exotic clusters (Ar, Xe) that were formed during rapid cooling resulting from the adiabatic expansion of gases issuing from jet sources under high pressure. An exception is provided by Ref. [130], where HHG is analyzed in substantially larger aggregates (aerogels).

The physical nature of this process in gas clusters is described primarily by the standard theory of HHG in atomic media with small modifications caused by the circumstance that the atoms in the clusters are close to each other. The high-order harmonics observed in this case are characterized by some increase in the conversion efficiency in comparison with that in atomic media. In that case, a certain difficulty is obvious in analyzing the spatial characteristics of such clusters and determining the percentage of nanoparticles in the volume where HHG occurred. Quite natural in this connection was a proposal to use commercially available nanoparticles, whose parameters could be determined with a high precision. Such structures may be used as targets for producing nanoparticle-containing plasma plumes.

In this section, we discuss the use of silver nanoparticles for enhancing the high-order nonlinear optical response (in particular, in HHG) in strong light fields. Nanoparticle parameters were analyzed used a scanning electron microscope prior to HHG experiments. These measurements showed that the nanoparticle diameter varied between 80 and 160 nm, with the average value 110 nm. The nanoparticles were glued to different surfaces. Prior to the experiments, it was verified that harmonic generation from the substances in contact with these clusters (droplets of glue, adhesive tape, glass surface) was ineffective in comparison with the HHG in plasmas containing silver nanoparticles. To compare the frequency conversion efficiency for laser radiation of atoms and nanoparticles containing the same atoms, experiments were conducted using both silver nanoparticles and a silver plate. At the first stage, HHG was optimized in the plasma produced on a silver plate. Subsequently, the targets were changed in order to investigate the generation of harmonics in the plasma containing silver nanoparticles under the same experimental conditions.

Figure 17 shows the intensity distribution for harmonics of the orders from 21 to 29 for plasma plumes containing silver atoms and nanoparticles. These investigations demonstrated a sixfold HHG efficiency increase in the nanoparticle-containing plasma in comparison the HHG efficiency in the plasma containing atoms of the same substance under the same experimental conditions. The conversion efficiency for the nanoparticle-containing plasma was estimated on the basis of the previous measurements of the conversion efficiency in a plasma produced on the surface of a silver plate (8×10^{-6}). Proceeding from a sixfold excess of harmonic energy in the case of a nanoparticle-containing medium, the HHG efficiency was estimated as 4×10^{-5} [54].

Comparing the H_c parameter for the two media with atomic and nanostructured particles revealed a small increase in this parameter with the use of nanoparticles. Up to 67th-order harmonics ($E_{ph} = 103$ eV) were obtained in the latter case, while H_c was equal to 61 ($E_{ph} = 94$ eV) in the case of a silver target. A similar insignificant increase in the highest harmonic order was earlier observed in the comparison of HHG in Ar clusters and in atomic argon [63]. In Ref. [63], the H_c value corresponded to the 33rd harmonic for a cluster-containing medium and to the 29th harmonic for a monomer medium (argon atoms). The difference in H_c was attributed to the higher electron affinity energy in the clusters. The high value of this parameter permits clusters (unlike atomic systems) to withstand ionization in the laser field even for high intensities, which in turn entails an increase in H_c.

In experiments with silver targets, the harmonic generation using an Ag plate was stable and did not require changing

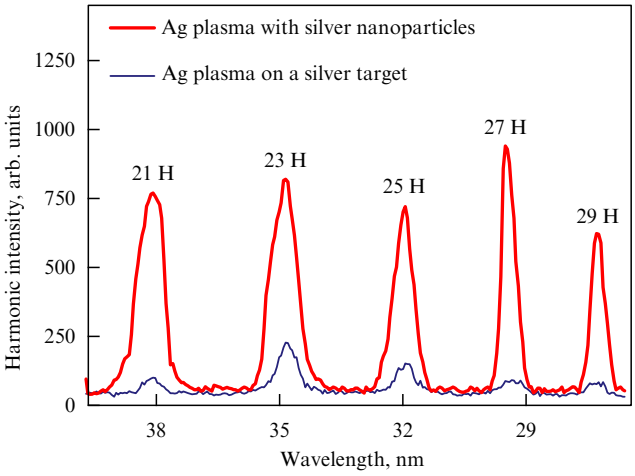

Figure 17. Harmonic distribution in the medium part of the plateau for a short delay between pulses for a plasma produced on the surface of a silver plate (thin curve) and a plasma containing silver nanoparticles (thick curve).

the target position for a long time for the pulse repetition rate 10 Hz. A different picture was observed for silver nanoparticle-bearing targets. Owing to rapid evaporation and a small amount of this material on the substrate surface, the harmonic generation was especially efficient for several initial laser shots; subsequently, the conversion efficiency decreased due to a substantial reduction of the active material (silver nanoparticles) in the region of femtosecond pulse transit. Figure 18a shows the HHG efficiency lowering with each successive laser shot when the target was not displaced during the experiment. The first laser shot was accompanied by a high-efficiency HHG with a typical plateau-like harmonic distribution beginning from the 17th-order harmonic. The subsequent shots on the surface of a target with nanoparticles and the corresponding conversion in the generated plasma were accompanied by a sharp decrease in the HHG efficiency, down to a complete disappearance of harmonics from the observed spectrum.

The observation described above permits an approximate reconstruction of the ablation picture for a target with nanoparticles. Silver nanoparticles were immediately surrounded by a polymer (epoxy resin, glue) that has a substantially lower fusion and evaporation heat than the material of a continuous (bulk) metallic target. As a result, the polymer begins to evaporate under substantially lower prepulse energies and in doing so entrains the surrounding silver nanoparticles. Multiple irradiation of this kind of target changed its parameters, led to a depletion of the nanoparticle content, a corresponding decrease in the nanoparticle density in the plume, and a decrease in the harmonic conversion efficiency under irradiation by subsequent pulses. Due to such an abrupt change in the conditions for harmonic generation in the medium with a depletion of the active particle density, determining the HHG efficiency as a function of the prepulse and main pulse parameters presented a serious problem. Nevertheless, estimative measurements of harmonic energies as functions of the intensity of the main pulse in the silver nanoparticle-containing plasma revealed a saturation of this process for moderate intensities of the femtosecond pulse ($I_{fp} \sim 8 \times 10^{14}$ W cm^{-2}).

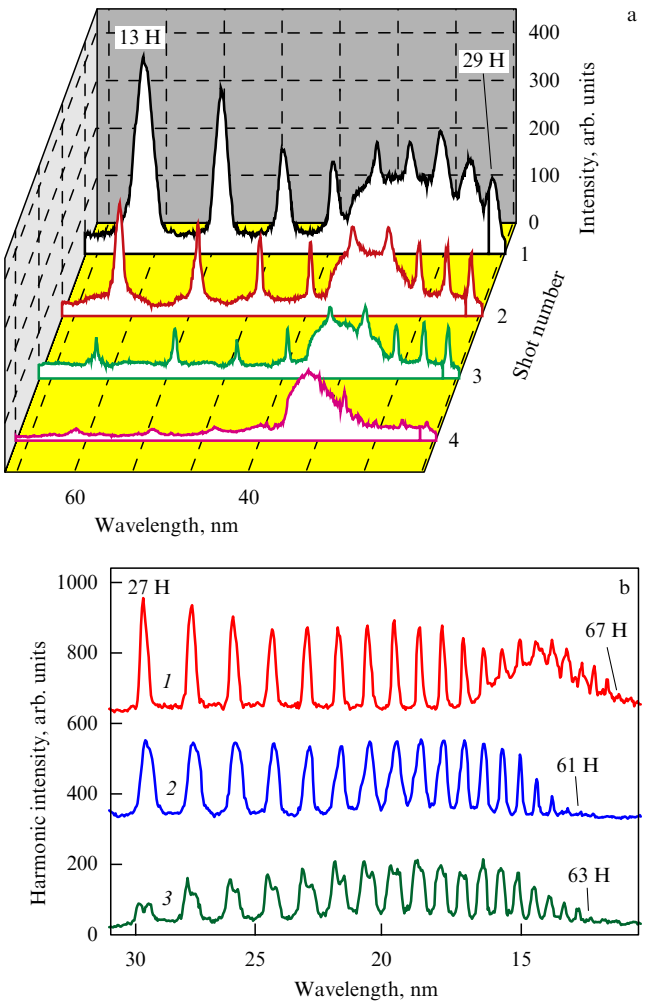

Figure 18. (a) Variation in the harmonic spectrum obtained in silver nanoparticle-containing plasma, with each successive laser shot. (b) High-order harmonic spectra generated in plasmas containing 110 nm silver particles (1), silver atoms (2), and 100–2000 nm blocks of silver atoms (3).

To analyze the effect of dimensional nanoparticle characteristics on HHG, comparison experiments were staged with plasmas that contained silver nanoblocks varying from 100 to 2000 nm in size. A plasma with such structures was generated on the surface of a target containing colloidal silver with nanoparticles of different sizes, which was confirmed by preliminary structural studies with the help of a scanning electron microscope. These investigations showed that the efficiency of harmonic generation in such nanoclusters (characterized by a substantial spread in dimensions and a diversity in geometrical shapes) was much lower than the efficiency of the above experiments with smaller nanoparticles (which were spherically shaped thereto). Figure 18b shows the harmonic spectrum generated in a plasma containing 100 – 2000 nm silver particles; also shown for comparison are the harmonic spectra generated in plasmas containing 110 nm spherical nanoparticles and silver atoms. These investigations demonstrated the adverse effect of increasing the cluster dimensions on the output characteristics of converted radiation for submicrometer dimensions of these particles. An increase in the particle size, on the one hand, involves an increase in its polarizability, which determines the efficiency of laser frequency conversion [66]. On the other hand, increasing the nanoparticle size entails a lowering of the HHG efficiency due to the involvement of only the surface atoms in the harmonic generation, reabsorption of the harmonics, recombination of electrons from the inner regions of the cluster, etc.

Recent investigations of other nanoparticles conducted to assess the feasibility of using them as a nonlinear medium for HHG revealed similar properties as with silver nanoparticles. In particular, the use of barium titanate (150 nm) and strontium titanate (38 nm) nanoparticles enabled generating harmonics with about the same highest orders as with solid-state analogues of these targets [131]. At the same time, the relatively large dimensions of these nanoparticles precluded the possibility of attaining conditions whereby the harmonics generated in the plasma containing these clusters would have higher intensities than the harmonics generated in plasmas containing monoatoms and ions of barium titanate and strontium titanate.

A qualitatively different picture was observed with the use of nanoparticles having typical dimensions 3 – 6 nm [132]. In this case, the harmonic intensities were observed to be appreciably higher than those generated in plasmas containing atoms and ions of the same materials (Fig. 19). This increase in the conversion efficiency may be attributed to the

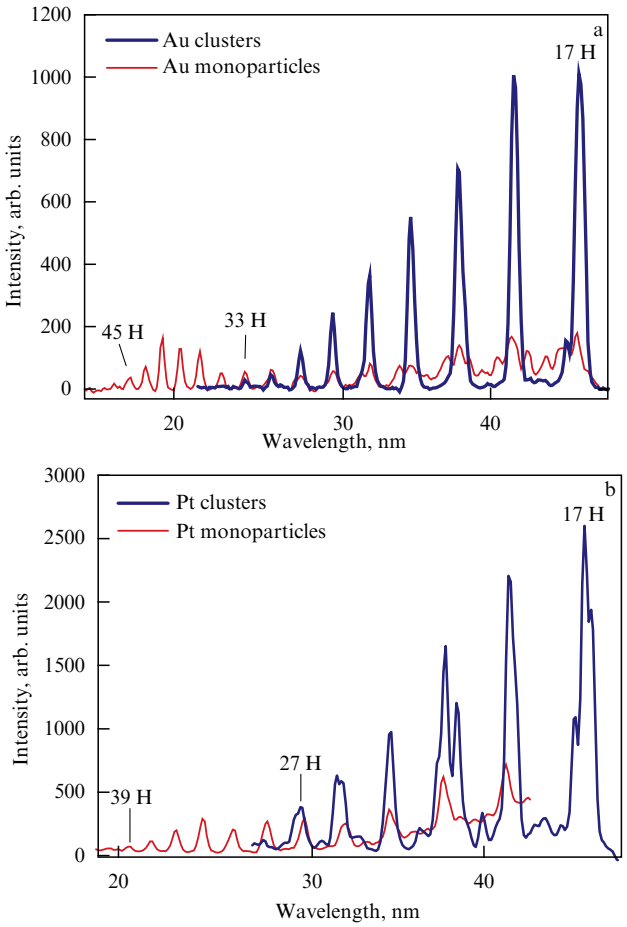

Figure 19. (a) High-order harmonic spectra obtained from plasmas containing 6nm gold clusters (bold curve) and gold monoparticles (thin curve). (b) High-order harmonic spectra obtained from plasmas containing 3 nm platinum clusters (bold curve) and platinum monoparticles (thin curve).

increase in the effective cross section for accelerated-electron capture by the nanoparticles. At the same time, the above adverse factors limiting the efficiency of HHG in clusters of larger size play a less significant role for such nanoparticles [133].

These HHG investigations involving cluster media demonstrated that their use does not result in an appreciable increase in the highest generated harmonic order. At the same time, a substantial increase in the harmonic conversion efficiency in comparison with that for plasma plumes containing ions and atoms of the same materials was observed in experiments.

In Ref. [63], which reports on a comparison of HHG in aggregated clusters and atoms of argon, it is shown that a medium of nanoparticles containing several thousand rare-gas atoms is more efficient from the harmonic generation standpoint than a medium of isolated atoms of a gas with the same density. A fivefold increase in the efficiency was obtained in experiments with gas clusters for harmonics of the orders from 3 to 9. Meanwhile, higher enhancement coefficients, notably in the shorter-wavelength domain (between the 17th and 23rd harmonics), were obtained in HHG in plasma media containing metal clusters (see Figs 17 and 19). These investigations also revealed a stronger dependence of the HHG efficiency on the prepulse and main pulse intensities of nanoparticles in comparison with that for monoparticles.

Here, an important point is the problem of geometrical nanoparticle parameter variations resulting from laser ablation. In this case, one might expect both aggregation and decomposition of clusters as a result of their melting in the interaction of high-power laser pulses with a nanoparticle-bearing surface. In the experiments outlined above, the presence of silver nanoparticles with initial geometrical parameters in the plasma was confirmed by analyzing the spatial characteristics of the material deposited on a nearby substrate in the course of laser ablation. At the same time, it would be desirable to carry out additional investigations of the components in a plasma produced by laser ablation of the nanoparticle-bearing surface in order to clarify the structure of clusters in the plume at the instant of femtosecond radiation transit.

The question of the advantages and disadvantages of using clusters as the nonlinear medium for high-order harmonic generation is still open. The experimental data given in this section familiarize the reader with the current state of affairs in this area of research into optical nanoparticle nonlinearities. HHG in cluster plasma media produced by the laser ablation of nanoparticle-bearing targets is analyzed in greater detail in review [134]. Here, we emphasize the following. Although several experimental parameters are controlled insufficiently well (in particular, cluster fragmentation or cluster aggregation fractions in the prepulse-induced ablation of nanoparticle-bearing targets), the data outlined signify that further investigations into HHG in cluster media hold good promise. Fullerenes may turn out to be an interesting object from this standpoint: they have a surface plasmon resonance in the 20 eV energy region, which gives hope for realizing enhanced nonlinear optical response in this spectral region (this applies, in particular, to the 13th and neighboring-order harmonics of titanium–sapphire laser radiation). Preliminary data show that these suggestions may be realized under certain fullerene excitation conditions.

9. Summary

The recent research described in this paper has led to a substantial improvement in HHG in laser-produced plasma and to an increase in the highest generated harmonic order in comparison with those obtained in earlier papers in this area. Figure 20 shows the best results attained early in plasma HHG investigations (plots *1–8*) and the data of recent investigations of harmonic generation in low-excited plasmas (plots *9–10*). In this case, the efficiency of conversion to harmonics in the plateau region was higher than 10^{-5}. It is noteworthy that in the early stages of research on HHG in gas-jet sources, the efficiency of this process did not exceed 10^{-6} in the same harmonic distribution range. More recently, the conversion efficiency was somewhat improved (up to 10^{-5}) owing to a better phase matching between the harmonic waves and the pump radiation. In the case of HHG from surfaces, whereby both odd and even harmonics are generated, the efficiency of conversion to low-order harmonics is much higher than that in HHG in gases or in a laser-produced plume. However, owing to a sharp surface HHG efficiency decrease with each subsequent harmonic order, the efficiency of this technique in the XUV range becomes comparable with the efficiency for isotropic media (gases and laser-produced plasma) or turns out to be lower

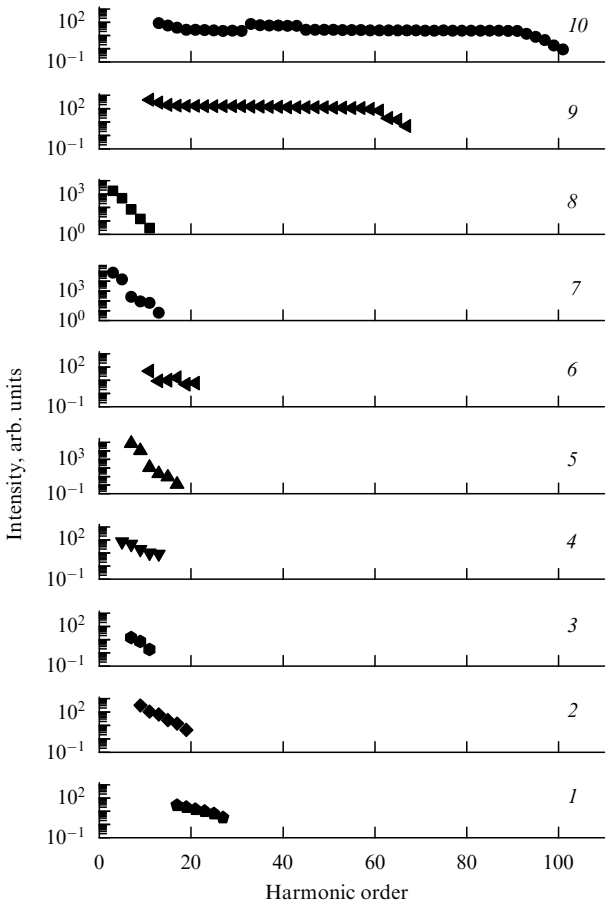

Figure 20. High-order harmonic spectra obtained from laser-produced plasma at the early stage of this research (1–8) and obtained in the investigations described in this review employing low excited and weakly ionized plasmas (9, 10). *1* — K II [19], *2* — LiF II [22], *3* — Na II [17], *4* — C II [20], *5* — C II [18], *6* — Pb III [18], *7* — Li II [17], *8* — Al II [21], *9* — Ag II [99], *10* — Mn III [41].

than that. We emphasize that forming resonance conditions that afford an increase in the efficiency for individual harmonics in the plateau region (up to 10^{-4}, which exceeds all previously attained values of the efficiency in the XUV range), allows substantially improving the energy characteristics of coherent XUV pulses for the purpose of using this radiation in different areas (nonlinear spectroscopy, attosecond physics, microlithography, biological applications, nanostructuring of objects, etc.). Using nanoparticles also permits improving the efficiency of HHG in laser-produced plasmas.

Among the main achievements in the investigations of the nonlinear optical properties of laser produced plasma, we note the relatively high generated harmonic orders (up to the 101st order, $\lambda = 7.9$ nm). The occurrence of a plateau-like harmonic distribution permits obtaining harmonics of about the same intensity in a broad XUV range. The HHG efficiency demonstrated for several plasma media (especially with noble metal targets) allows using this radiation not only for the above purposes but also for its further conversion to a shorter-wavelength spectral range, as well as generating harmonic series and pulses of attosecond duration. Experiments of this kind are now in the preparatory stage. The capability of enhancing only one harmonic (rather than a series of harmonics) permits employing these radiation sources without the preliminary spectral selection accomplished with dispersion elements and filters (which lead to an appreciable loss of the pulse energy). In sight is the quest for similar resonance mechanisms in an even shorter-wavelength domain than that where an enhancement of an individual harmonic has been realized to date. The presently accumulated understanding of the plasma processes occurring in HHG gives hope for a further improvement of frequency-converted radiation characteristics.

This paper is based on an analysis of HHG experiments conducted using a low-excited laser-produced plasma, which have demonstrated several new approaches to the problem of increasing the HHG efficiency in comparison with the efficiency of conventional HHG in gases. At the same time, it is obvious that gas HHG exhibits much higher harmonic orders (in comparison with the plasma HHG data outlined in this paper). Without making excessively optimistic predictions that the orders of in-plasma-generated harmonics will exceed the gas harmonic orders in the near future, we have focused the reader's attention primarily on the realization of new techniques for increasing the frequency-converted radiation intensity with the use of plasma plumes, which may hardly be realized in standard gas HHG.

From future investigations, we may expect an improvement of plasma HHG due to a double excitation of laser-produced plasmas, an optimization of the longitudinal harmonic generation scheme in the laser plume, an optimization of nanostructured plasmas, the use of multicomponent plasma plumes, the formation of quasiphase-matching conditions for the waves, the provision of a regime of waveguide pump propagation through the plasma medium, the feasibility analysis of attosecond pulse generation in laser-produced plasma, etc. It follows from the above that investigations in this area of nonlinear optics are making rapid strides and may bring new success in the near future.

Acknowledgements. The author expresses his appreciation to his numerous colleagues, with whom most of the investigations presented in this paper were carried out. A special acknowledgment is due to H Kuroda, P D Gupta, P A Naik, and T Ozaki for the fruitful discussions of different aspects of harmonic generation in laser-produced plasmas. The author also expresses his gratitude to many participants in these investigations (M Suzuki, H Singhal, L B Elouga Bom, J A Chakera, M Baba, U Chakravarty, I A Kulagin, P V Red'kin, R A Khan, M Raghuramaiah, and V Arora) for their cooperation.

References

1. Tsakiris G D et al. *New J. Phys.* **8** 19 (2006)
2. Dromey B et al. *Nature Phys.* **2** 456 (2006)
3. Reitze D H et al. *Opt. Lett.* **29** 86 (2004)
4. Pfeifer T et al. *Appl. Phys. B* **80** 277 (2005)
5. Froud C A et al. *Opt. Lett.* **31** 374 (2006)
6. Gibson E A et al. *Science* **302** 95 (2003)
7. Kazamias S et al. *Phys. Rev. Lett.* **90** 193901 (2003)
8. Teubner U et al. *Phys. Rev. A* **67** 013816 (2003)
9. Norreys P A et al. *Phys. Rev. Lett.* **76** 1832 (1996)
10. Pert G J *Phys. Rev. A* **75** 023808 (2007)
11. Ozaki T et al. *Phys. Rev. Lett.* **89** 253902 (2002)
12. Grüner F et al. *Appl. Phys. B* **86** 431 (2007)
13. Corkum P B, Krausz F *Nature Phys.* **3** 381 (2007)
14. Figueira de Morisson Faria C et al. *Phys. Rev. A* **65** 023404 (2002)
15. Taïeb R et al. *Phys. Rev. A* **68** 033403 (2003)

16. Silin V P, Silin P V *Usp. Fiz. Nauk* **177** 763 (2007) [*Phys. Usp.* **50** 729 (2007)]
17. Akiyama Y et al. *Phys. Rev. Lett.* **69** 2176 (1992)
18. Kubodera S et al. *Phys. Rev. A* **48** 4576 (1993)
19. Wahlström C-G et al. *Phys. Rev. A* **51** 585 (1995)
20. Theobald W et al. *Opt. Commun.* **120** 177 (1995)
21. Ganeev R A, Redkorechev V I, Usmanov T *Opt. Commun.* **135** 251 (1997)
22. Krushelnick K, Tighe W, Suckewer S *J. Opt. Soc. Am. B* **14** 1687 (1997)
23. Corkum P B *Phys. Rev. Lett.* **71** 1994 (1993)
24. Gladkov S M, Koroteev N I *Usp. Fiz. Nauk* **160** (7) 105 (1990) [*Sov. Phys. Usp.* **33** 554 (1990)]
25. Gladkov S M et al. *Pis'ma Zh. Tekh. Fiz.* **14** 1399 (1988) [*Sov. Tech. Phys. Lett.* **14** 610 (1988)]
26. Fedotov A B et al. *J. Opt. Soc. Am. B* **8** 363 (1991)
27. Fedotov A B, Koroteev N I, Zheltikov A M *Laser Phys.* **5** 835 (1995)
28. Fedotov A B et al. *Opt. Commun.* **133** 587 (1997)
29. Ganeev R A et al. *Appl. Opt.* **45** 748 (2006)
30. Ganeev R et al. *Opt. Lett.* **30** 768 (2005)
31. Ganeev R A et al. *Opt. Lett.* **31** 1699 (2006)
32. Ganeev R A et al. *Phys. Rev. A* **74** 063824 (2006)
33. Ganeev R A et al. *J. Appl. Phys.* **99** 103303 (2006)
34. Ganeev R A et al. *Opt. Lett.* **32** 65 (2007)
35. Ganeev R A et al. *Appl. Phys. B* **81** 1081 (2005)
36. Ganeev R A et al. *J. Opt. Soc. Am. B* **23** 2535 (2006)
37. Suzuki M et al. *Opt. Lett.* **31** 3306 (2006)
38. Suzuki M et al. *Opt. Express* **15** 1161 (2007)
39. Ganeev R A et al. *Appl. Phys. B* **87** 243 (2007)
40. Suzuki M et al. *Opt. Express* **15** 4112 (2007)
41. Ganeev R A et al. *Phys. Rev. A* **76** 023831 (2007)
42. Ganeev R A et al. *Phys. Lett. A* **339** 103 (2005)
43. Seres E, Seres J, Spielmann C *Appl. Phys. Lett.* **89** 181919 (2006)
44. Krause J L, Schafer K J, Kulander K C *Phys. Rev. Lett.* **68** 3535 (1992)
45. Lewenstein M et al. *Phys. Rev. A* **49** 2117 (1994)
46. Milošević D B *J. Opt. Soc. Am. B* **23** 308 (2006)
47. Milošević D B *J. Phys. B*: *At. Mol. Opt. Phys.* **40** 3367 (2007)
48. Milošević D B *J. Phys. B*: *At. Mol. Opt. Phys.* **33** 2479 (2000)
49. Fischer R, Lein M, Keitel C H *J. Phys. B: At. Mol. Opt. Phys.* **40** F113 (2007)
50. Reagan B A et al. *Phys. Rev. A* **76** 013816 (2007)
51. Cohen O et al. *Phys. Rev. Lett.* **98** 043903 (2007)
52. von der Linde D et al. *Phys. Rev. A* **52** R25 (1995)
53. Tarasevitch A et al. *Phys. Rev. Lett.* **98** 103902 (2007)
54. Ganeev R A *J. Phys. B*: *At. Mol. Opt. Phys.* **40** R213 (2007)
55. Gibbon P *Short Pulse Laser Interactions with Matter*: *An Introduction* (London: Imperial College Press, 2005)
56. von der Linde D, Rzàżewski K *Appl. Phys. B* **63** 499 (1996)
57. Jaeglé P *Coherent Sources of XUV Radiation*: *Soft X-Ray Lasers and High-Order Harmonic Generation* (New York: Springer, 2006)
58. Milošević D B, Ehlotzky F *Adv. At. Mol. Opt. Phys.* **49** 373 (2003)
59. Antoine P et al. *Phys. Rev. A* **53** 1725 (1996)
60. Miyazaki K, Takada H *Phys. Rev. A* **52** 3007 (1995)
61. Christov I P, Murnane M M, Kapteyn H C *Phys. Rev. Lett.* **78** 1251 (1997)
62. Tempea G et al. *Phys. Rev. Lett.* **84** 4329 (2000)
63. Donnelly T D et al. *Phys. Rev. Lett.* **76** 2472 (1996)
64. Hu S X, Xu Z Z *Appl. Phys. Lett.* **71** 2605 (1997)
65. Ivanov M Yu, Corkum P B *Phys. Rev. A* **48** 580 (1993)
66. Liang Y et al. *J. Phys. B*: *At. Mol. Opt. Phys.* **27** 5119 (1994)
67. Ganeev R A et al. *J. Opt. Soc. Am. B* **24** 1319 (2007)
68. Kuroda H et al. *Laser Part. Beams* **23** 183 (2005)
69. Ganeev R A et al. *J. Opt. Soc. Am. B* **24** 1138 (2007)
70. Ganeev R A et al. *Phys. Rev. A* **76** 023832 (2007)
71. Ozaki T et al. *Laser Part. Beams* **25** 321 (2007)
72. Suzuki M et al. *J. Opt. Soc. Am. B* **24** 2686 (2007)
73. Ganeev R A, Elouga Bom L B, Ozaki T *Appl. Phys. Lett.* **91** 131104 (2007)
74. Ganeev R A, Elouga Bom L B, Ozaki T *J. Appl. Phys.* **102** 073105 (2007)
75. Ganeev R A et al. *J. Opt. Soc. Am. B* **24** 3823 (2007)
76. Reintjes J F *Nonlinear Optical Parametric Processes in Liquids and Gases* (New York: Academic Press, 1984)
77. Gaarde M B, Schafer K J *Phys. Rev. A* **64** 013820 (2001)
78. Toma E S et al. *J. Phys. B*: *At. Mol. Opt. Phys.* **32** 5843 (1999)
79. Zeng Z et al. *Phys. Scripta* **66** 321 (2002)
80. Bartels R et al. *Nature* **406** 164 (2000)
81. Kim H T et al. *Phys. Rev. A* **69** 031805 (2004)
82. Duffy G, Dunne P *J. Phys. B*: *At. Mol. Opt. Phys.* **34** L173 (2001)
83. Ganeev R A et al. *Appl. Phys. Lett.* **86** 131116 (2005)
84. Singhal H et al. *J. Appl. Phys.* **103** 013107 (2008)
85. D'Arcy R et al. *J. Phys. B*: *At. Mol. Opt. Phys.* **32** 4859 (1999)
86. Ganeev R A et al. *Phys. Rev. A* **75** 063806 (2007)
87. Duffy G, van Kampen P, Dunne P *J. Phys. B*: *At. Mol. Opt. Phys.* **34** 3171 (2001)
88. Dunne P et al. *J. Phys. B*: *At. Mol. Opt. Phys.* **32** L597 (1999)
89. Suzuki M et al. *Appl. Phys. Lett.* **90** 261104 (2007)
90. Ganeev R A, Redkin P V *Opt. Commun.* **281** 4126 (2008)
91. Suzuki M et al. *Phys. Lett. A* **372** 4480 (2008)
92. Ganeev R A, Milošević D B *J. Opt. Soc. Am. B* **25** 1127 (2008)
93. Balcou P, L'Huillier A *Phys. Rev. A* **47** 1447 (1993)
94. Reintjes J, She C-Y, Eckardt R *IEEE J. Quantum Electron.* **14** 581 (1978)
95. Pfeifer T et al. *Opt. Lett.* **31** 975 (2006)
96. Ishikawa K L, Takahashi E J, Midorikawa K *Phys. Rev. A* **75** 021801 (2007)
97. Zeng Z et al. *Phys. Rev. Lett.* **98** 203901 (2007)
98. Ozaki T et al. *Laser Part. Beams* **25** 321 (2007)
99. Elouga Bom L B et al. *Phys. Rev. A* **75** 033804 (2007)
100. Ganeev R A et al. *Eur. Phys. J. D* **37** 255 (2006)
101. Kim H T, Tosa V, Nam C H *J. Phys. B*: *At. Mol. Opt. Phys.* **39** S265 (2006)
102. Tosa V et al. *Phys. Rev. A* **67** 063817 (2003)
103. Brimhall N et al. *Opt. Express* **15** 1684 (2007)
104. Larsen J T, Lane S M *J. Quant. Spectrosc. Radiat. Transf.* **51** 179 (1994)
105. Rubenchik A M et al. *Appl. Surf. Sci.* **127 – 129** 193 (1998)
106. Wood-Vasey W M et al. *Laser Part. Beams* **18** 583 (2000)
107. Tillack M S et al. *J. Phys. IV* (France) **133** 985 (2006)
108. Ganeev R A et al. *J. Opt. Soc. Am. B* **24** 2770 (2007)
109. Suzuki M et al. *J. Opt. Soc. Am. B* **24** 2847 (2007)
110. Ganeev R A et al. *J. Opt. Soc. Am. B* **23** 1332 (2006)
111. Ganeev R A et al. *Phys. Rev. A* **76** 023805 (2007)
112. Tosa V et al. *Phys. Rev. A* **71** 063807 (2005)
113. Ganeev R A et al. *J. Opt. Soc. Am. B* **22** 1927 (2005)
114. Ganeev R A, Kuroda H *Opt. Commun.* **256** 242 (2005)
115. Ganeev R A et al. *J. Mod. Opt.* **53** 1451 (2006)
116. Ganeev R A et al. *Opt. Commun.* **249** 569 (2005)
117. Liao H B et al. *Appl. Phys. B* **65** 673 (1997)
118. Shvetsov-Shilovski N I et al. *Laser Phys. Lett.* **4** 726 (2007)
119. Tisch J W G et al. *J. Phys. B*: *At. Mol. Opt. Phys.* **30** L709 (1997)
120. Vozzi C et al. *Appl. Phys. Lett.* **86** 111121 (2005)
121. Pai C-H et al. *Opt. Lett.* **31** 984 (2006)
122. Tisch J W G *Phys. Rev. A* **62** 041802 (2000)
123. Véniard V, Taïeb R, Maquet A *Phys. Rev. A* **65** 013202 (2001)
124. Vázquez de Aldana J R, Roso L *J. Opt. Soc. Am. B* **18** 325 (2001)
125. Kundu M, Popruzhenko S V, Bauer D *Phys. Rev. A* **76** 033201 (2007)
126. Shim B et al. *Phys. Rev. Lett.* **98** 123902 (2007)
127. Tajima T, Kishimoto Y, Downer M C *Phys. Plasmas* **6** 3759 (1999)
128. Fomyts'kyi M V et al. *Phys. Plasmas* **11** 3349 (2004)
129. Fomichev S V et al. *Phys. Rev. A* **71** 013201 (2005)
130. Flettner A et al. *Appl. Phys. B* **77** 747 (2003)
131. Ganeev R A et al. *J. Opt. Soc. Am. B* **25** 325 (2008)
132. Ganeev R A et al. *J. Appl. Phys.* **103** 063102 (2008)
133. Ganeev R A et al. *J. Phys. B*: *At. Mol. Opt. Phys.* **41** 045603 (2008)
134. Ganeev R A *Laser Phys.* **18** 1009 (2008)